5 Theory of elasticity in three dimensions

After the one-dimensional applications of chapter 2 and the two-dimensional plate problems of the chapters 3 and 4, a generalisation to three dimensions will be made.
In a space continuum the displacement of a point (x, y, z) in a cartesian coordinate system, can be decomposed into the components $u_x(x, y, z)$ in the x-direction, $u_y(x, y, z)$ in the y-direction and $u_z(x, y, z)$ in the z-direction. Per unit of volume the external loads P_x, P_y and P_z can be applied, which correspond with the degrees of freedom u_x, u_y and u_z, respectively. Regarding the internal quantities, it already was demonstrated that a surface element in a continuum is able to transmit a force per unit of area and that this force per unit of area was called a stress vector. In a space continuum, the stress vectors acting in arbitrary direction on three areas that are perpendicular to the cartesian coordinate axes x, y, z can be decomposed into three components along these three coordinate directions. Doing so, nine quantities appear indicated by $\sigma_{xx}, \sigma_{xy}, \sigma_{xz}$ (acting on the area perpendicular to the x-axis), $\sigma_{yx}, \sigma_{yy}, \sigma_{yz}$ (acting on the area perpendicular to the y-axis) and $\sigma_{zx}, \sigma_{zy}, \sigma_{zz}$ (acting on the area perpendicular to the z-axis). Again it can be seen that the first subscript of the stress components (often just called stresses) indicates the direction of the normal on the area, and the second subscript the direction of the component of the stress vector. Similarly as in the plate theory, a stress component is called a normal stress when the two indices are equal $(\sigma_{xx}, \sigma_{yy}, \sigma_{zz})$. When the indices are different they are called shear stresses $(\sigma_{xy}, \sigma_{xz}, \sigma_{yx}, \sigma_{yz}, \sigma_{zx}, \sigma_{zy})$. Also in this case the sign convention holds that a stress component is positive when it is working in positive coordinate direction on an area with its normal in positive coordinate direction.
With the defined internal stress components, internal deformation components correspond. These are known as specific strains caused by the normal stresses and changes of the right angle due to the shear stresses.
As indicated in Fig. 5.1, the specific strains associated with the normal stresses are called $\varepsilon_{xx}, \varepsilon_{yy}, \varepsilon_{zz}$, respectively. The shear deformations consist out of three pairs of equal angular

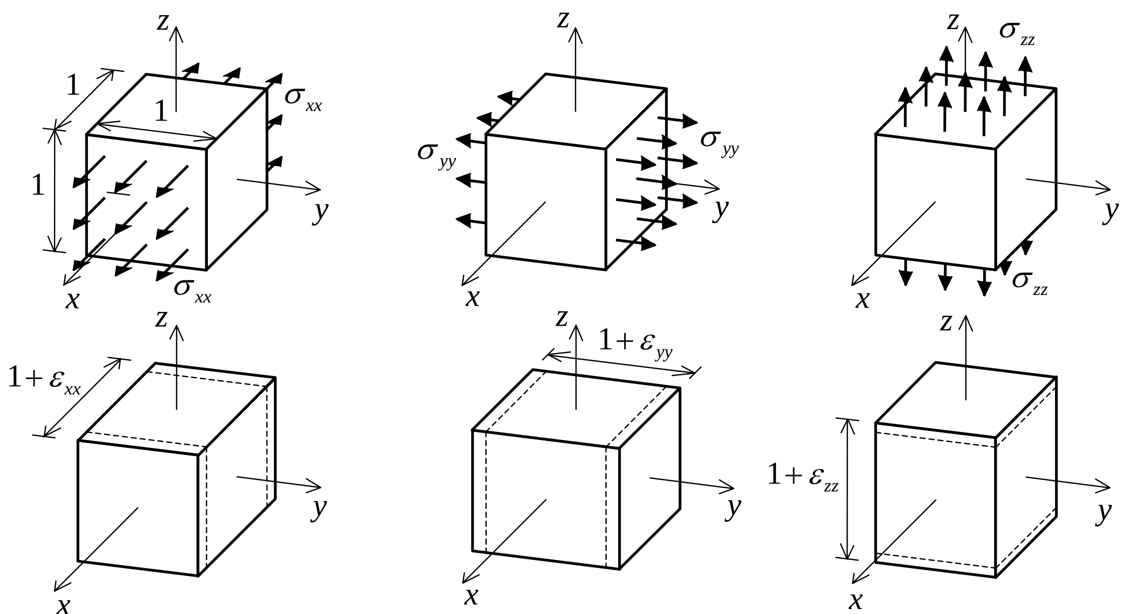

Fig. 5.1: Positive normal stresses with corresponding strains in a three-dimensional continuum.

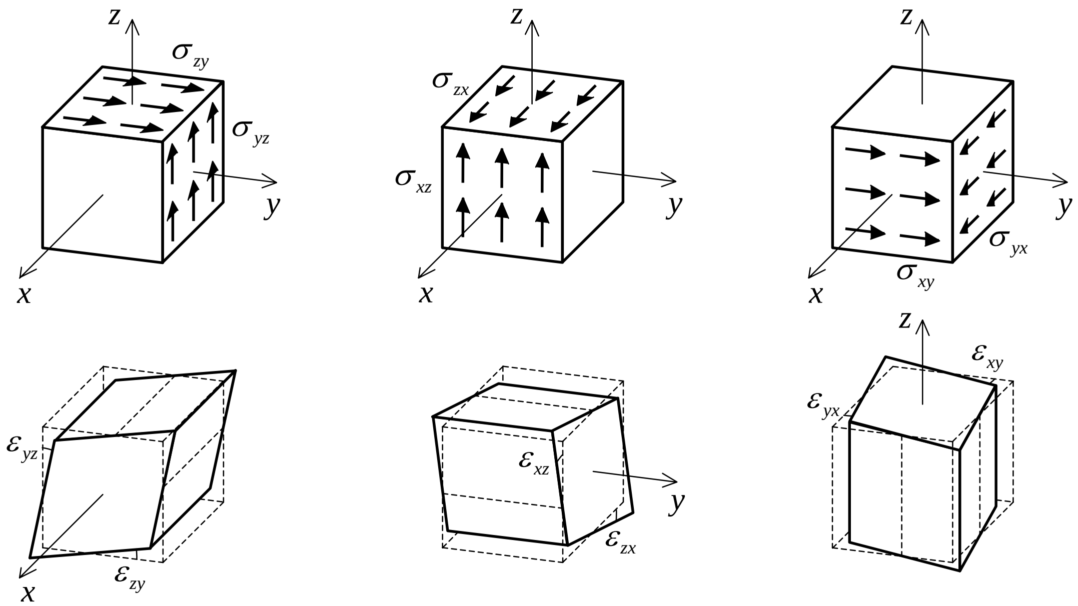

Fig. 5.2: Positive shear stresses with corresponding strains in a three-dimensional continuum.

changes $\varepsilon_{yz} = \varepsilon_{zy}$, $\varepsilon_{xz} = \varepsilon_{xz}$, $\varepsilon_{xy} = \varepsilon_{yx}$ (see Fig. 5.2). As done before, the shear deformations can be used, which are defined by: $\gamma_{yz} = 2\varepsilon_{yz}$, $\gamma_{zx} = 2\varepsilon_{zx}$, $\gamma_{xy} = 2\varepsilon_{xy}$. Then the scheme of relations as shown in Fig. 5.3 can be set up.
Since six stress components are present and only three load components (i.e. three equilibrium equations) a three-dimensional stress problem is statically indeterminate to the third degree.

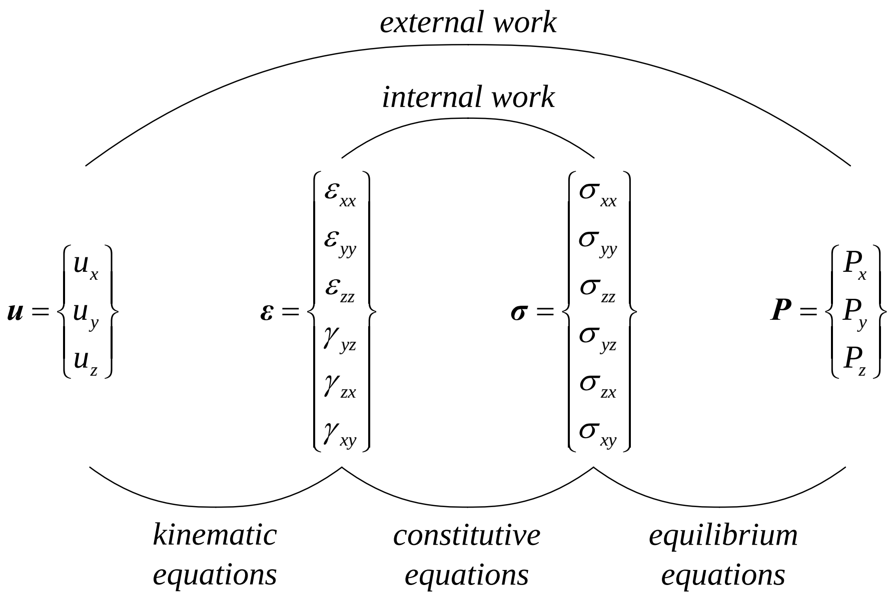

Fig. 5.3: Diagram displaying the relations between the quantities playing a role in the analysis of three-dimensional problems.

5.1 Basic equations

Subsequently the three categories of basic equations will be formulated in the following order: kinematic equations, constitutive equations and equilibrium equations.

Kinematic equations
In section 3.1, the kinematic equations for a plate were derived. Similarly by considerations in three directions, the kinematic equations for a space continuum are found:

$$\boxed{\begin{array}{lll} \varepsilon_{xx} = u_{x,x} & ; & \gamma_{yz} = 2\,\varepsilon_{yz} = u_{y,z} + u_{z,y} \\ \varepsilon_{yy} = u_{y,y} & ; & \gamma_{zx} = 2\,\varepsilon_{zx} = u_{z,x} + u_{x,z} \\ \varepsilon_{zz} = u_{z,z} & ; & \gamma_{xy} = 2\,\varepsilon_{xy} = u_{x,y} + u_{y,x} \end{array}} \tag{5.1}$$

In this notation, the subscript "$,x$" means differentiation with respect to x, etc.
In addition to deformations, a volume particle can also be subjected to a displacement as a rigid body. Six displacement components exist. Three of them are pure translations u_x, u_y, u_z in x-, y-, z- directions, respectively. The other three are rotations about the x-, y-, z- axes. They are called $\omega_{yz}, \omega_{zx}, \omega_{xy}$, respectively.

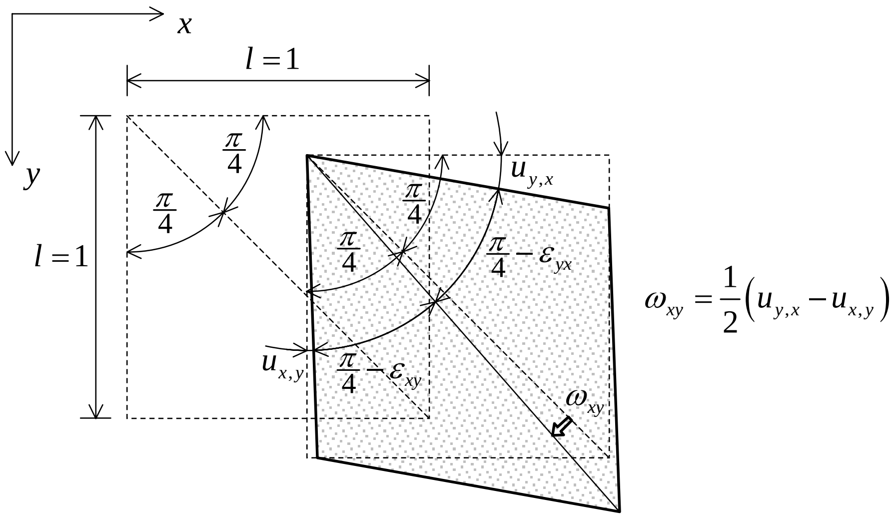

Fig. 5.4: Rotation about z-axis.

Fig. 5.4 shows the rotation ω_{xy} about the z-axis. Doing so, for the three rotations it is found (anticlockwise is positive):

$$\boxed{\begin{array}{l} \omega_{yz} = \frac{1}{2}\left(u_{z,y} - u_{y,z}\right) \\ \omega_{zx} = \frac{1}{2}\left(u_{x,z} - u_{z,x}\right) \\ \omega_{xy} = \frac{1}{2}\left(u_{y,x} - u_{x,y}\right) \end{array}} \tag{5.2}$$

Constitutive equations

Hooke's law is valid for an isotropic linear-elastic material. The stress-strain relations are:

$$\boxed{\begin{aligned}
\varepsilon_{xx} &= \frac{1}{E}\sigma_{xx} - \frac{\upsilon}{E}\left(\sigma_{yy}+\sigma_{zz}\right) \quad ; \quad 2\varepsilon_{yz} = \frac{2(1+\upsilon)}{E}\sigma_{yz} \\
\varepsilon_{yy} &= \frac{1}{E}\sigma_{yy} - \frac{\upsilon}{E}\left(\sigma_{zz}+\sigma_{xx}\right) \quad ; \quad 2\varepsilon_{zx} = \frac{2(1+\upsilon)}{E}\sigma_{zx} \\
\varepsilon_{zz} &= \frac{1}{E}\sigma_{zz} - \frac{\upsilon}{E}\left(\sigma_{xx}+\sigma_{yy}\right) \quad ; \quad 2\varepsilon_{xy} = \frac{2(1+\upsilon)}{E}\sigma_{xy}
\end{aligned}} \tag{5.3}$$

where E is the *modulus of elasticity* (*Young's modulus*) and υ *Poisson's ratio* (*lateral contraction coefficient*). The term $2(1+\upsilon)/E$ is the reciprocal quantity of the shear modulus G. The matrix formulation of the constitutive equations read:

$$\boxed{\begin{Bmatrix}\varepsilon_{xx}\\ \varepsilon_{yy}\\ \varepsilon_{zz}\\ \gamma_{yz}\\ \gamma_{zx}\\ \gamma_{xy}\end{Bmatrix} = \frac{1}{E}\begin{bmatrix}1 & -\upsilon & -\upsilon & 0 & 0 & 0\\ & 1 & -\upsilon & 0 & 0 & 0\\ & & 1 & 0 & 0 & 0\\ & & & 2(1+\upsilon) & 0 & 0\\ & symmetrical & & & 2(1+\upsilon) & 0\\ & & & & & 2(1+\upsilon)\end{bmatrix}\begin{Bmatrix}\sigma_{xx}\\ \sigma_{yy}\\ \sigma_{zz}\\ \sigma_{yz}\\ \sigma_{zx}\\ \sigma_{xy}\end{Bmatrix}} \tag{5.4)a$$

or briefly:

$$\boxed{\boldsymbol{\varepsilon} = \boldsymbol{C}\,\boldsymbol{\sigma}} \tag{5.4)b$$

where $\boldsymbol{C}$ is called the *flexibility matrix* or *compliance matrix*.

Through inversion, the stiffness formulation of the constitutive equations appears:

$$\boxed{\begin{Bmatrix}\sigma_{xx}\\ \sigma_{yy}\\ \sigma_{zz}\\ \sigma_{yz}\\ \sigma_{zx}\\ \sigma_{xy}\end{Bmatrix} = \frac{(1-\upsilon)E}{(1+\upsilon)(1-2\upsilon)}\begin{bmatrix}1 & \frac{\upsilon}{1-\upsilon} & \frac{\upsilon}{1-\upsilon} & 0 & 0 & 0\\ & 1 & \frac{\upsilon}{1-\upsilon} & 0 & 0 & 0\\ & & & 0 & 0 & 0\\ & & & \frac{1-2\upsilon}{2(1-\upsilon)} & 0 & 0\\ & & & & \frac{1-2\upsilon}{2(1-\upsilon)} & 0\\ & & symmetrical & & & \frac{1-2\upsilon}{2(1-\upsilon)}\end{bmatrix}\begin{Bmatrix}\varepsilon_{xx}\\ \varepsilon_{yy}\\ \varepsilon_{zz}\\ \gamma_{yz}\\ \gamma_{zx}\\ \gamma_{xy}\end{Bmatrix}} \tag{5.5)a$$

or briefly:

$$\boxed{\boldsymbol{\sigma} = \boldsymbol{D}\,\boldsymbol{\varepsilon}} \tag{5.5)b$$

where $\boldsymbol{D}$ is called the *stiffness matrix* or *rigidity matrix*.
In this formulation the constitutive equations are normally used in the finite element programmes with spatial elements.

Equilibrium equations
In Fig. 5.5 the equilibrium in x-direction is considered. The edges of the drawn cube have unit length. Similarly the equilibrium in the y- and z-directions can be set up. Doing so, it can be derived:

$$\boxed{\begin{aligned} \sigma_{xx,x} + \sigma_{yx,x} + \sigma_{zx,z} + P_x = 0 \\ \sigma_{xy,x} + \sigma_{yy,y} + \sigma_{zy,z} + P_y = 0 \\ \sigma_{xz,x} + \sigma_{yz,y} + \sigma_{zz,z} + P_z = 0 \end{aligned}} \tag{5.6)a$$

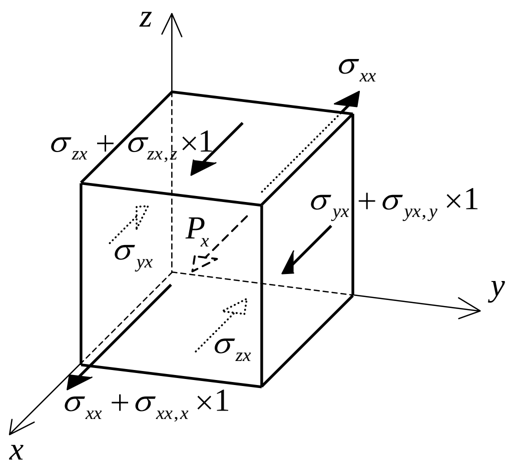

Fig. 5.5: Forces in x-direction.

Equilibrium of moments about the x-, y- and z-axis leads to:

$$\boxed{\sigma_{yz} = \sigma_{zy} \quad ; \quad \sigma_{zx} = \sigma_{xz} \quad ; \quad \sigma_{xy} = \sigma_{yx}} \tag{5.6)b$$

Check with matrices of differential operators
For the kinematic equations it can be written:

$$\boxed{\begin{Bmatrix} \varepsilon_{xx} \\ \varepsilon_{yy} \\ \varepsilon_{zz} \\ \gamma_{yz} \\ \gamma_{zx} \\ \gamma_{xy} \end{Bmatrix} = \begin{bmatrix} \frac{\partial}{\partial x} & 0 & 0 \\ 0 & \frac{\partial}{\partial y} & 0 \\ 0 & 0 & \frac{\partial}{\partial z} \\ 0 & \frac{\partial}{\partial z} & \frac{\partial}{\partial y} \\ \frac{\partial}{\partial z} & 0 & \frac{\partial}{\partial x} \\ \frac{\partial}{\partial y} & \frac{\partial}{\partial x} & 0 \end{bmatrix} \begin{Bmatrix} u_x \\ u_y \\ u_z \end{Bmatrix}} \tag{5.7)a$$

or briefly:

$$\boxed{\boldsymbol{\varepsilon} = \mathcal{B}\, \boldsymbol{u}} \tag{5.7)b$$

Likewise, the equilibrium equations (5.6)a in this notation read:

$$\boxed{\begin{bmatrix} -\frac{\partial}{\partial x} & 0 & 0 & 0 & -\frac{\partial}{\partial z} & -\frac{\partial}{\partial y} \\ 0 & -\frac{\partial}{\partial y} & 0 & -\frac{\partial}{\partial z} & 0 & -\frac{\partial}{\partial x} \\ 0 & 0 & -\frac{\partial}{\partial z} & -\frac{\partial}{\partial y} & -\frac{\partial}{\partial x} & 0 \end{bmatrix} \begin{Bmatrix} \sigma_{xx} \\ \sigma_{yy} \\ \sigma_{zz} \\ \sigma_{yz} \\ \sigma_{zx} \\ \sigma_{xy} \end{Bmatrix} = \begin{Bmatrix} P_x \\ P_y \\ P_z \end{Bmatrix}} \tag{5.8)a$$

or briefly:

$$\boxed{\mathcal{B}' \boldsymbol{\sigma} = \boldsymbol{P}} \tag{5.8)b$$

Also in this case $\mathcal{B}'$ can be obtained by transposition of $\mathcal{B}$ plus the introduction of a minus sign for all uneven derivatives.

5.2 Solution procedures and boundary conditions

For the *force method*, one would expect three compatibility conditions. However, in literature continuously six compatibility conditions are derived. But these conditions are linearly independent, so that from the six conditions also three identities can be derived, the so-called identities of Bianchi. This means that in the three-dimensional analysis an extra complication arises, which is not present in the previously discussed one- and two-dimensional problems. In this Course, no further attention will be paid to this matter.
In the *displacement method*, the kinematic and the constitutive equations are substituted in the equilibrium equations. This approach results in a set of three simultaneous partial differential equations in the three components u_x, u_y and u_z of the displacement field:

$$\boxed{\begin{array}{l} \cdots u_x + \cdots u_y + \cdots u_z = P_x \\ \cdots u_x + \cdots u_y + \cdots u_z = P_y \\ \cdots u_x + \cdots u_y + \cdots u_z = P_z \end{array}} \qquad (5.9)$$

The positions indicated by the three dots are occupied by differential operators multiplied by the stiffness terms from (5.5). An alternative description of these three differential equations will be provided in section 5.5.

Remark
In this course, no general applications will be discussed for three-dimensional stress-states, which are described by the system of differential equations given by (5.9). Only one special case will be highlighted, the torsion of bars. Chapter 6 is completely dedicated to this problem. For the case of torsion, it appears that the three-dimensional stress-state can be reduced to a two-dimensional problem.

Boundary conditions
The general goal of the theory of elasticity can be described as follows:
The calculation of displacements, deformations and stresses inside a body, which is subjected to known volume forces and certain known conditions at its outer surface.
The most frequently appearing boundary conditions are:

Kinematic boundary conditions
This boundary condition occurs when at a specific part of the outer surface (say S_u), such a provision is made that the points of that part are subjected to a prescribed displacement. For example, a part of the body can be glued completely to a rigid supporting block. Then the displacements for the glued surface are zero (in other words: it is prescribed that the displacements are zero). The formulae for this type of boundary condition read:

$$
\left.\begin{aligned}
u_x &= u_x^o \\
u_y &= u_y^o \\
u_z &= u_z^o
\end{aligned}\right\} \text{ on } S_u \tag{5.10}
$$

where u_x^o, u_y^o and u_z^o are prescribed (for example zero).

Dynamic boundary conditions

This boundary condition occurs when at a specific part of the outer surface (say S_p) a certain surface load is acting. For that case, three relations can be formulated between the stress components with respect to the cartesian coordinate system. When the unit outward-pointing normal on the surface has the components e_x, e_y and e_z, the formulation of the boundary condition becomes:

$$
\left.\begin{aligned}
\sigma_{xx}e_x + \sigma_{yx}e_y + \sigma_{zx}e_z &= p_x \\
\sigma_{xy}e_x + \sigma_{yy}e_y + \sigma_{zy}e_z &= p_y \\
\sigma_{xz}e_x + \sigma_{yz}e_y + \sigma_{zz}e_z &= p_z
\end{aligned}\right\} \quad \text{on } S_p \tag{5.11}
$$

where p_x, p_y and p_z are prescribed. On an unloaded part of the surface p_x, p_y and p_z are zero of course.

The boundary conditions (5.11) are a generalisation into three dimensions of the corresponding conditions for a plate loaded in its plane. The derivation is performed analogously. A triangular surface element ABC with unit area as shown in Fig. 5.6 is

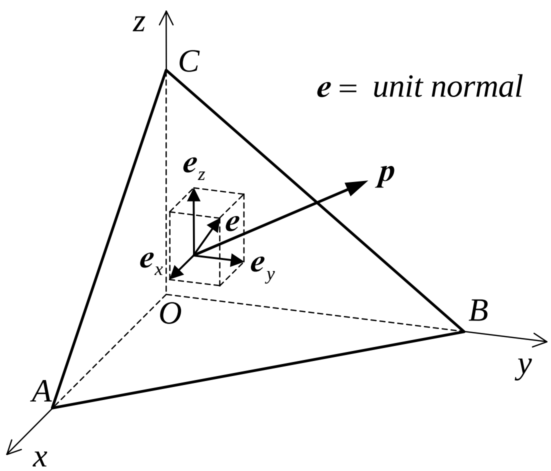

Fig. 5.6: Derivation of dynamic boundary conditions.

considered, on which a vector $\boldsymbol{p}$ is acting with components p_x, p_y and p_z. As mentioned before, the unit outward-pointing normal on ABC has the components e_x, e_y and e_z. From elementary stereometric principles it follows that the areas of triangles OBC, OAC and OAB are equal to e_x, e_y and e_z, respectively. By considering the equilibrium of the tetrahedron in the directions x, y and z, the three conditions of (5.11) can be derived.

Exercises

1. Find the deformation field corresponding with the following displacement field:
   $u_x = a + by \quad ; \quad u_y = c - b\,x \quad ; \quad u_z = d$
2. Determine the displacement field corresponding with the following (homogeneous) deformation field, when also is given that $u_z = 0$:
   $\varepsilon_{xx} = a \quad ; \quad \varepsilon_{yy} = b \quad ; \quad \varepsilon_{zz} = \varepsilon_{xy} = \varepsilon_{yz} = \varepsilon_{zx} = 0$
3. Is the following stress field possible, for a body in equilibrium without being subjected to volume loads?
   $\sigma_{xx} = a\,x^2 \quad ; \quad \sigma_{xy} = \sigma_{yx} = -2\,a\,x\,y \quad ; \quad \sigma_{yy} = a\,y^2 \quad ; \quad \sigma_{xz} = \sigma_{yz} = \sigma_{zx} = \sigma_{zy} = \sigma_{zz} = 0$
4. When in a body, which is in equilibrium, the following stresses are present (k, ρ and g are constants): $\sigma_{xx} = \sigma_{yy} = k\rho g\,z$; $\sigma_{zz} = \rho\,g\,z$; $\sigma_{xy} = \sigma_{xz} = \sigma_{yx} = \sigma_{yz} = \sigma_{zx} = \sigma_{zy} = 0$.
   Which volume force is acting on the body?

5.3 Alternative formulation of the constitutive equations

In section 5.1 Hooke's law was presented for the description of the behaviour of isotropic linear-elastic material. A relation was formulated between the six stress components σ_{xx}, σ_{yy}, σ_{zz}, σ_{yz}, σ_{zx}, σ_{xy} and the associated deformations ε_{xx}, ε_{yy}, ε_{zz}, ε_{yz}, ε_{zx}, ε_{xy}. This relation was presented in both flexibility and stiffness formulation. It appeared that the two elastic constants E and υ were sufficient for a unique description of the material behaviour. Sometimes it is advantageous, to adapt the description such that in the total deformation distinction can be made between the *change of volume* and the *change of shape*. For example for the behaviour of soil this may be important, where the change of volume is prevented by the pore water while the change of shape can take place unhampered. Then instead of the constants E and υ, two other constants are introduced. Another example is rubber, which is incompressible. This means that change of volume is zero and the value of υ is practically 0.5. In $(5.5)_a$ the term $(1-2\upsilon)$ that appears in the denominator makes the relation between stresses and strains undetermined. The splitting-up of the deformations causing a change of volume and a change of shape may simplify the description of the non-linear behaviour of materials. Among other things this is important for concrete and soil. In this section the alternative description of Hooke's law will be summarised. To start with, the law will be split up in a separate *law for the change of volume* and a *law for the change of shape*. This will be done in both the flexibility and stiffness formulations. Then two other material constants will be introduced, they are the *compression modulus* K and the *shear modulus* G. The starting point of the derivation is formed by the basic equations (5.4) and (5.5). Finally, for the two description methods, the two separate laws are combined to one total law of Hooke. Further, it appears that for the stiffness formulation another alternative exists, where the constants K and G are replaced by the so-called *constants of Lamé* λ and μ.

5.3.1 Separate laws of Hooke for the change of volume and shape

From the occurring stress-state given by the stress components σ_{xx}, σ_{yy}, σ_{zz}, σ_{yz}, σ_{zx}, σ_{xy} the so-called *hydrostatic stress* σ_0 is split off. The hydrostatic stress is defined by:

$$\boxed{\sigma_0 = \frac{1}{3}\left(\sigma_{xx} + \sigma_{yy} + \sigma_{zz}\right)} \tag{5.12}$$

The remaining stress components are the deviator stresses s_{xx}, s_{yy}, s_{zz}, σ_{yz}, σ_{zx}, σ_{xy}. For the first three components it holds:

$$\boxed{\begin{aligned} s_{xx} &= \sigma_{xx} - \sigma_0 = \frac{1}{3}\left(2\sigma_{xx} - \sigma_{yy} - \sigma_{zz}\right) \\ s_{yy} &= \sigma_{yy} - \sigma_0 = \frac{1}{3}\left(2\sigma_{yy} - \sigma_{zz} - \sigma_{xx}\right) \\ s_{zz} &= \sigma_{zz} - \sigma_0 = \frac{1}{3}\left(2\sigma_{zz} - \sigma_{xx} - \sigma_{yy}\right) \end{aligned}} \tag{5.13}$$

Analogously a component e_0 is split off from the existing deformations ε_{xx}, ε_{yy}, ε_{zz}, ε_{yz}, ε_{zx}, ε_{xy}, which is equal to one third of the *change of volume* e:

$$\boxed{e_0 = \frac{1}{3}\left(\varepsilon_{xx} + \varepsilon_{yy} + \varepsilon_{zz}\right) = \frac{1}{3}e} \tag{5.14}$$

Then the remaining part is formed by the *deviator deformations* e_{xx}, e_{yy}, e_{zz}, ε_{yz}, ε_{zx}, ε_{xy}. The first three components are:

$$\boxed{\begin{aligned} e_{xx} &= \varepsilon_{xx} - e_0 = \frac{1}{3}\left(2\varepsilon_{xx} - \varepsilon_{yy} - \varepsilon_{zz}\right) \\ e_{yy} &= \varepsilon_{yy} - e_0 = \frac{1}{3}\left(2\varepsilon_{yy} - \varepsilon_{zz} - \varepsilon_{xx}\right) \\ e_{zz} &= \varepsilon_{zz} - e_0 = \frac{1}{3}\left(2\varepsilon_{zz} - \varepsilon_{xx} - \varepsilon_{yy}\right) \end{aligned}} \tag{5.15}$$

No change of volume is associated with the six deviator deformations. It just changes the form (shape) of a material particle.

Flexibility relations

A relation can be established between e and σ_0 by adding up the first three equations of $(5.4)_a$. This delivers:

$$\varepsilon_{xx} + \varepsilon_{yy} + \varepsilon_{zz} = \frac{3(1-2\upsilon)}{E}\frac{1}{3}\left(\sigma_{xx} + \sigma_{yy} + \sigma_{zz}\right)$$

or:

$$\boxed{e = \frac{1}{K}\sigma_0}$$ (*Hooke's law for the change of volume in flexibility formulation*) (5.16)

with:

$$\boxed{K = \frac{E}{3(1-2\upsilon)}}$$ (*modulus of compression*) (5.17)

Relation (5.16) is Hooke's law for the change of volume. A relation can also be derived between the deviator deformations e_{xx}, e_{yy}, e_{zz} and the deviator stresses s_{xx}, s_{yy}, s_{zz}. For example from (5.15) it is known that $e_{xx} = \varepsilon_{xx} - e_0$, for both ε_{xx} and e_0 the relation with the stresses is known, so that:

$$e_{xx} = \frac{1}{E}\left(\sigma_{xx} - \upsilon\sigma_{yy} - \upsilon\sigma_{zz}\right) - \frac{1-2\upsilon}{3E}\left(\sigma_{xx} + \sigma_{yy} + \sigma_{zz}\right)$$

or:

$$e_{xx} = \frac{1+\upsilon}{E}\left(\frac{2}{3}\sigma_{xx} - \frac{1}{3}\sigma_{yy} - \frac{1}{3}\sigma_{zz}\right)$$

This expression can be briefly written as:

$$e_{xx} = \frac{1}{2G}s_{xx}$$

where G is the *shear modulus*. A similar derivation holds for the relations between e_{yy} and s_{yy}, and between e_{zz} and s_{zz}. The shear modulus also establishes a relation between the shear deformations γ_{yz}, γ_{zx}, γ_{xy} and the shear stresses σ_{yz}, σ_{zx}, σ_{yx}. When for the shear deformations the quantities ε_{yz}, ε_{zx}, ε_{xy} are used the factor $1/2G$ appears again. Therefore, for all six deviator deformations and stresses it holds:

$$\boxed{\begin{array}{lll} e_{xx} = \frac{1}{2G}s_{xx} & ; & \varepsilon_{yz} = \frac{1}{2G}\sigma_{yz} \\ e_{yy} = \frac{1}{2G}s_{yy} & ; & \varepsilon_{zx} = \frac{1}{2G}\sigma_{zx} \\ e_{zz} = \frac{1}{2G}s_{zz} & ; & \varepsilon_{xy} = \frac{1}{2G}\sigma_{xy} \end{array}}$$ (*Hooke's law for the change of shape in flexibility formulation*) (5.18)

with:

$$\boxed{G = \frac{E}{2(1+\upsilon)}} \qquad (\textit{shear modulus}) \qquad (5.19)$$

Stiffness relations

The two components (5.16) and (5.18) of Hooke's law can also be derived in inverse form as stiffness relations. By addition of the first three equations in $(5.5)_a$, and division of the result by three, it is found:

$$\frac{1}{3}\left(\sigma_{xx}+\sigma_{yy}+\sigma_{zz}\right)=\frac{E}{3(1-2\upsilon)}\left(\varepsilon_{xx}+\varepsilon_{yy}+\varepsilon_{zz}\right)$$

which is just equal to:

$$\boxed{\sigma_0 = K\,e} \qquad (\textit{Hooke's law for the change of volume in stiffness formulation}) \qquad (5.20)$$

The relation between the deviator stresses s_{xx}, s_{yy}, s_{zz} and the deviator strains e_{xx}, e_{yy}, e_{zz} can simply be obtained. For s_{xx} it is known that $s_{xx}=\sigma_{xx}-\sigma_0$. Substitution of σ_{xx} and σ_0 as functions of the deformations then yields:

$$s_{xx}=\frac{(1-\upsilon)E}{(1+\upsilon)(1-2\upsilon)}\left(\varepsilon_{xx}+\frac{\upsilon}{1-\upsilon}\varepsilon_{yy}+\frac{\upsilon}{1-\upsilon}\varepsilon_{zz}\right)-\frac{E}{3(1-2\upsilon)}\left(\varepsilon_{xx}+\varepsilon_{yy}+\varepsilon_{zz}\right)$$

After some elaboration this reduces to:

$$s_{xx}=\frac{E}{(1+\upsilon)}\left(\frac{2}{3}\varepsilon_{xx}-\frac{1}{3}\varepsilon_{yy}-\frac{1}{3}\varepsilon_{zz}\right)$$

which briefly can be written as:

$$s_{xx}=2G\,e_{xx}$$

Analogously similar expressions are found for s_{yy} and s_{zz}. Therefore, Hooke's law for the change of shape in stiffness form reads:

$$\boxed{\begin{array}{lll} s_{xx}=2G\,e_{xx} & ; & \sigma_{yz}=2G\,\varepsilon_{yz} \\ s_{yy}=2G\,e_{yy} & ; & \sigma_{zx}=2G\,\varepsilon_{zx} \\ s_{zz}=2G\,e_{zz} & ; & \sigma_{xy}=2G\,\varepsilon_{xy} \end{array}} \qquad (\textit{Hooke's law for the change of shape in stiffness formulation}) \qquad (5.21)$$

5.3.2 Hooke's law for total deformations and stresses

With the two separate laws of Hooke on basis of K and G for the change of volume and shape, respectively, a general law on basis of K and G can be formulated for the total deformations (in flexibility formulation), or for the total stresses (in stiffness formulation).

Flexibility relations

The total strains ε_{xx}, ε_{yy}, ε_{zz}, ε_{yz}, ε_{zx}, ε_{xy} are the sum of the average strain $e_0 = \frac{1}{3}e$ and the deviator deformations e_{xx}, e_{yy}, e_{zz}, ε_{yz}, ε_{zx}, ε_{xy}. With the relations (5.16) and (5.18) it then directly can be found:

$$\boxed{\begin{aligned} \varepsilon_{xx} &= \frac{\sigma_0}{3K} + \frac{s_{xx}}{2G} \quad ; \quad \varepsilon_{yz} = \frac{\sigma_{yz}}{2G} \\ \varepsilon_{yy} &= \frac{\sigma_0}{3K} + \frac{s_{yy}}{2G} \quad ; \quad \varepsilon_{zx} = \frac{\sigma_{zx}}{2G} \\ \varepsilon_{zz} &= \frac{\sigma_0}{3K} + \frac{s_{zz}}{2G} \quad ; \quad \varepsilon_{xy} = \frac{\sigma_{xy}}{2G} \end{aligned}} \qquad \text{(*Hooke's law in K and G for the total deformations in flexibility formulation*)} \qquad (5.22)$$

Stiffness relations

The total stresses σ_{xx}, σ_{yy}, σ_{zz}, σ_{yz}, σ_{zx}, σ_{xy} are the sum of the hydrostatic stress σ_0 and the deviator stresses s_{xx}, s_{yy}, s_{zz}, σ_{yz}, σ_{zx}, σ_{xy}. With the relation (5.20) and (5.21), for the total stresses it then directly can be found:

$$\boxed{\begin{aligned} \sigma_{xx} &= K\,e + 2G\,e_{xx} \quad ; \quad \sigma_{yz} = 2G\,\varepsilon_{yz} \\ \sigma_{yy} &= K\,e + 2G\,e_{yy} \quad ; \quad \sigma_{zx} = 2G\,\varepsilon_{zx} \\ \sigma_{zz} &= K\,e + 2G\,e_{zz} \quad ; \quad \sigma_{xy} = 2G\,\varepsilon_{xy} \end{aligned}} \qquad \text{(*Hooke's law in K and G for the total stresses in stiffness formulation*)} \qquad (5.23)$$

This law for the total stresses in stiffness formulation, can also be represented in a different manner. The three deviator deformations e_{xx}, e_{yy}, e_{zz} are replaced by $\varepsilon_{xx} - \frac{1}{3}e$, $\varepsilon_{yy} - \frac{1}{3}e$, $\varepsilon_{zz} - \frac{1}{3}e$, respectively. The law then becomes:

$$\boxed{\begin{aligned} \sigma_{xx} &= \lambda\,e + 2\mu\,\varepsilon_{xx} \quad ; \quad \sigma_{yz} = 2\mu\,\varepsilon_{yz} \\ \sigma_{yy} &= \lambda\,e + 2\mu\,\varepsilon_{yy} \quad ; \quad \sigma_{zx} = 2\mu\,\varepsilon_{zx} \\ \sigma_{zz} &= \lambda\,e + 2\mu\,\varepsilon_{zz} \quad ; \quad \sigma_{xy} = 2\mu\,\varepsilon_{xy} \end{aligned}} \qquad \text{(*Hooke's law in } \lambda \text{ and } \mu \text{ for the total stresses in stiffness formulation*)} \qquad (5.24)$$

where λ and μ are called the Lamé constants. These constants can be expressed in K and G and also in E and υ. The following expressions are valid:

$$\lambda = K - \frac{2}{3}G = \frac{\upsilon E}{(1+\upsilon)(1-2\upsilon)} \quad ; \quad \mu = G = \frac{E}{2(1+\upsilon)} \qquad (5.25)$$

The quantity μ is identical to G, but it is customary to use μ in combination with λ.

5.3.3 The displacement method in the description of Lamé

In section 5.2 it has been discussed that the displacement method for three-dimensional problems amounts to the simultaneous solution of three partial differential equations in u_x, u_y and u_z (see (5.9)).
These three differential equations can be formulated very concisely, if Hooke's law is expressed in the Lamé constants λ and μ.
The three sets basic equations then are:

$$\begin{array}{ll} \varepsilon_{xx} = u_{x,x} & ; \quad \varepsilon_{yz} = \frac{1}{2}\left(u_{y,z} + u_{z,y}\right) \\ \varepsilon_{yy} = u_{y,y} & ; \quad \varepsilon_{zx} = \frac{1}{2}\left(u_{z,x} + u_{x,z}\right) \\ \varepsilon_{zz} = u_{z,z} & ; \quad \varepsilon_{xy} = \frac{1}{2}\left(u_{x,y} + u_{y,x}\right) \end{array} \qquad \text{(\textit{kinematic equations})}$$

$$\begin{array}{ll} \sigma_{xx} = \lambda e + 2\mu\varepsilon_{xx} & ; \quad \sigma_{yz} = 2\mu\varepsilon_{yz} \\ \sigma_{yy} = \lambda e + 2\mu\varepsilon_{yy} & ; \quad \sigma_{zx} = 2\mu\varepsilon_{zx} \\ \sigma_{zz} = \lambda e + 2\mu\varepsilon_{zz} & ; \quad \sigma_{xy} = 2\mu\varepsilon_{xy} \end{array} \qquad \text{(\textit{constitutive equations})}$$

$$\begin{array}{l} \sigma_{xx,x} + \sigma_{yx,y} + \sigma_{zx,z} + P_x = 0 \\ \sigma_{xy,x} + \sigma_{yy,y} + \sigma_{zy,z} + P_y = 0 \\ \sigma_{xz,x} + \sigma_{yz,y} + \sigma_{zz,z} + P_z = 0 \end{array} \qquad \text{(\textit{equilibrium equations})}$$

By downward substitution the three equilibrium equations are transformed into the so-called equations of Navier:

$$\begin{array}{l} (\lambda + \mu)e_{,x} + \mu\nabla^2 u_x + P_x = 0 \\ (\lambda + \mu)e_{,y} + \mu\nabla^2 u_y + P_y = 0 \\ (\lambda + \mu)e_{,z} + \mu\nabla^2 u_z + P_z = 0 \end{array} \qquad \text{(\textit{equations of Navier})} \qquad (5.26)$$

where the volume strain e is a function of the displacements and ∇^2 is the Laplace operator for three dimensions, i.e.:

$$e = u_{x,x} + u_{y,y} + u_{z,z} \quad ; \quad \nabla^2 = \frac{\partial^2}{\partial x^2} + \frac{\partial^2}{\partial y^2} + \frac{\partial^2}{\partial z^2}$$

Use of tensor notation
A big advantage in the formulation of above relations can be obtained by the use of the index notation including summation convention. To start with, the coordinate axes x, y, z are indicated by x_1, x_2, x_3, respectively. The displacement components then are u_1, u_2, u_3. The stress components are σ_{ij} $(i, j = 1, 2, 3)$ and the strain components are ε_{ij} $(i, j = 1, 2, 3)$. The notation for partial differentiation is:

$$a_{,i} = \frac{\partial a}{\partial x_i}$$

The summation convention of Einstein requires that when in an expression one subscript appears twice, a summation has to be carried out with respect to this index from 1 to 3, i.e.:

$$a_{ii} = \sum_{i=1}^{3} a_{ii} = a_{11} + a_{22} + a_{33}$$

Another useful quantity is the Kronecker delta, defined by:

$$\delta_{ij} = \begin{cases} 1 & \text{when} \quad i = j \\ 0 & \text{when} \quad i \neq j \end{cases}$$

The three sets of basic equations now become:

$$\boxed{\begin{array}{ll} e_{ij} = \frac{1}{2}\left(u_{i,j} + u_{j,i}\right) & (i, j = 1, 2, 3) \\ \sigma_{ij} = 2\mu\,\varepsilon_{ij} + \lambda\,\varepsilon_{kk}\,\delta_{ij} & (i, j = 1, 2, 3) \\ \sigma_{ij,i} + P_j = 0 & (j = 1, 2, 3) \end{array}} \quad \begin{array}{l} (\textit{kinematic equations}) \\ (\textit{constitutive equations}) \\ (\textit{equilibrium equations}) \end{array} \tag{5.27}$$

Downward substitution again provides the equations of Navier:

$$\boxed{(\lambda + \mu)\,u_{j,ji} + \mu\,u_{i,jj} + P_i = 0 \quad (i = 1, 2, 3)} \tag{5.28}$$

The boundary conditions are:

$$\boxed{\begin{array}{lll} u_i = u_i^0 & \text{on } S_p & (i = 1, 2, 3) \\ \sigma_{ij} e_i = p_j & \text{on } S_0 & (j = 1, 2, 3) \end{array}} \tag{5.29}$$

The advantage of this notation is that the whole system of equations can be written very concisely and simple. Substitution of one equation into another can be done as well. In literature this notation is used intensively.

6 Torsion of bars

6.1 Problem definition

During the civil engineering training at the university, the student is thoroughly introduced in the behaviour of bar structures. The student has been familiarised with the basic cases of *extension*, *bending*, *shear*, *torsion* and their combinations. For each basic case, two external quantities can be identified, namely a specific deformation and a corresponding generalised stress resultant. For the case of extension they are ε and N, for bending κ and M, for shear γ and V and for torsion θ and M_t.
From each of the four basic cases, for the designer always two specifications are important. First, he has to know the *stiffness*. This is the relation between the specific deformation and the corresponding stress resultant. For the several cases the relations are:

$$N = EA\varepsilon \qquad (\textit{extension})$$
$$M = EI\,\kappa \qquad (\textit{bending})$$
$$V = GA_s\,\gamma \qquad (\textit{shear})$$
$$M_t = GI_t\,\theta \qquad (\textit{torsion})$$

Here is EA the axial stiffness, EI the bending stiffness, GA_s the shear stiffness and GI_t the torsional stiffness. The quantity E is the *modulus of elasticity* (also called *Young's modulus*) and G is the *shear modulus*. The quantities A, I, A_s and I_t follow from the shape of the cross-section of the bar. The area A and the bending moment of inertia I of the cross-section do not need extra explanation. The quantity A_s is the cross-sectional area to be applied for shear; only for circular cross-sections this area is equal to A. The quantity I_t is called the torsional moment of inertia. During previous courses a lot of attention is paid to the determination of A and I, and to a less extend to A_s. Compared to this, the torsional problem was summarily dealt with. In previous lectures, only for a number simple cases a solution has been derived, but a generally valid analysis has not been provided up to now.
As mentioned, a second quantity in each of the basic cases is important for the designer. This is information about the *stress distribution* over the cross-section. For the case of extension the stress is constant, for bending the stress varies linearly, and for shear the stresses can be derived from the stress distribution for bending via an equilibrium consideration. The stress distribution for torsion has been derived only for the above-mentioned simple special cases. A generally valid procedure has not been presented yet. In summary, for the stress calculation the following is known:

$$N = \sigma A \qquad (\textit{extension})$$
$$M = \sigma W \qquad (\textit{bending})$$
$$V = \sigma \frac{bI}{S} \qquad (\textit{shear})$$
$$M_t = \ ? \qquad (\textit{torsion})$$

Here is A the cross-sectional area, W the section factor, I the bending moment of inertia, b the width subjected to the shear stress σ and S the static moment of a part of the cross-section. The stiffness problems and the stress distributions are shown schematically in Fig. 6.1. For the case of torsion, the only thing that can be established is that the torsional moment M_t has to be obtained from the integration over the cross-section of the product of the shear stress σ and the lever arm r.

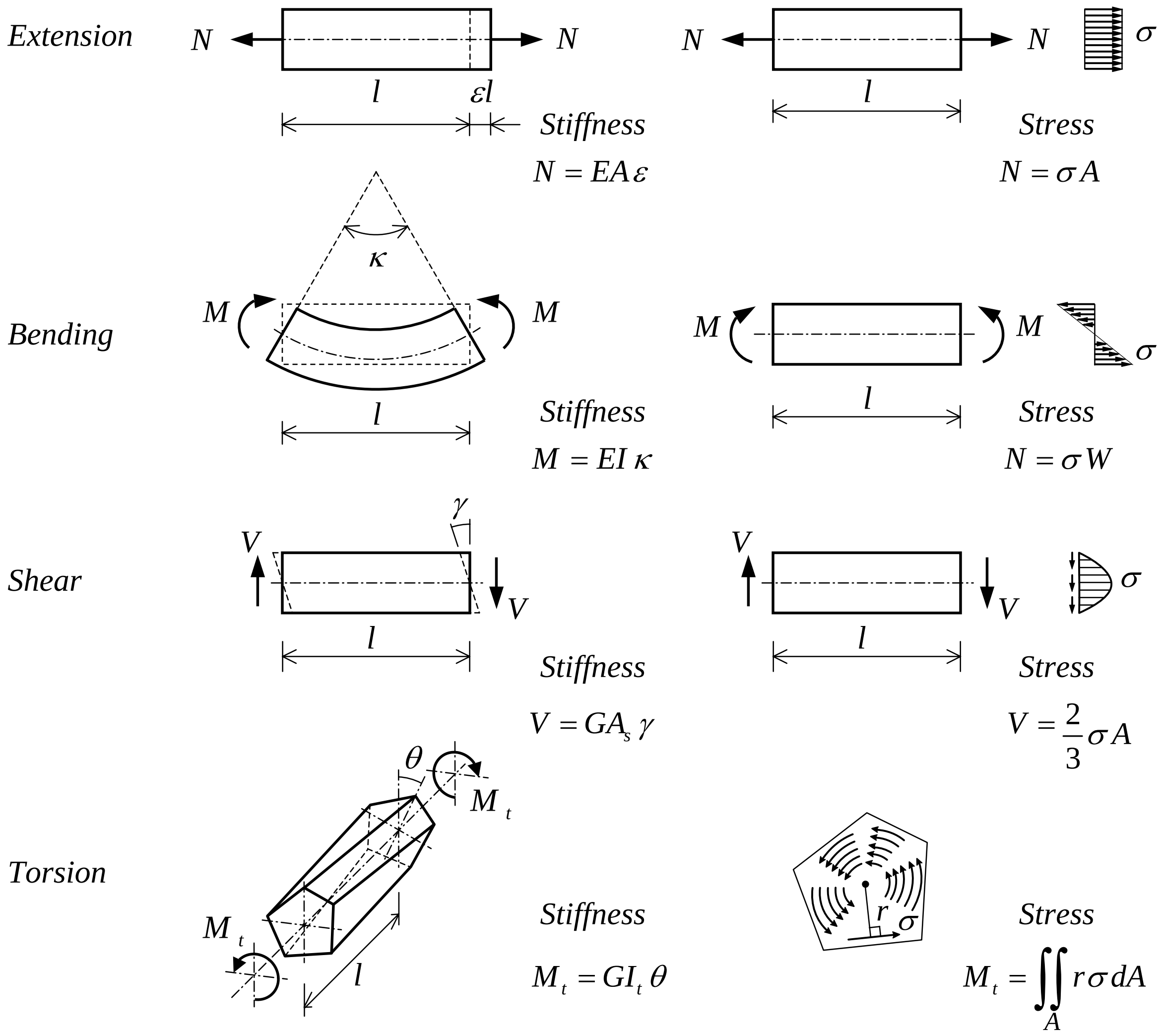

Fig.6.1: Definition of stiffness and stress distribution for the four basic load cases of a bar.

Before this problem definition is concluded, the three simple special cases of torsion are mentioned, for which the solution was generated in previous courses. It only concerned prismatic bars of circular cross-section, strip-shaped cross-section and thin-walled hollow cross-section. The found relations for the torsional moments of inertia I_t and the maximum occurring stresses are indicated in Fig. 6.2.
The main goal of this chapter is to offer a generally valid theory for prismatic bars with arbitrarily shaped cross-sections. These cross-sections may be solid but may contain holes as well. In the case of hollow cross-sections, the wall thickness not necessarily needs to be small. Attention is also paid to the possibility of cross-sections composed out of two different materials. Fig. 6.3 provides an overview of the cross-sections to be considered.

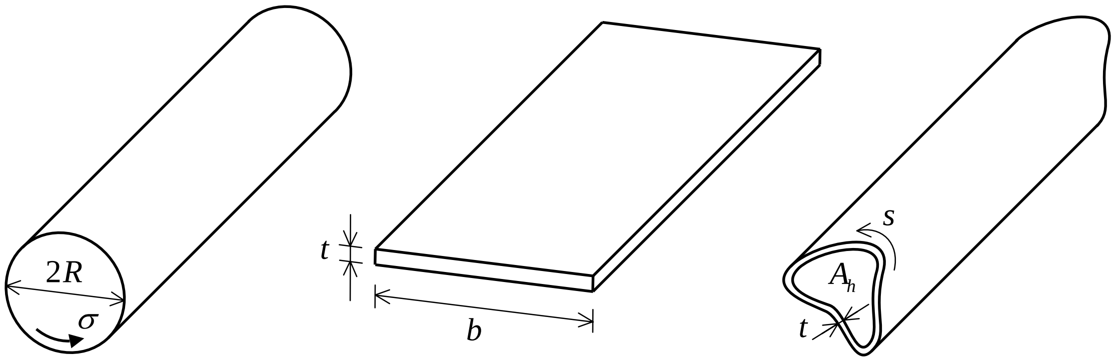

$$I_t = \frac{1}{2}\pi R^4 \qquad I_t = \frac{1}{3} b t^3 \qquad I_t = \frac{4A_h^2}{\oint \frac{ds}{t}} = \frac{4t\,A_h^2}{C}$$

$$\sigma = \frac{M_t}{\frac{1}{2}\pi R^3} \qquad \sigma = \frac{M_t}{\frac{1}{3} b t^2} \qquad \sigma = \frac{M_t}{2t A_h}$$

Fig. 6.2: Torsional moment of inertia I_t and shear stress σ for simple special cases.

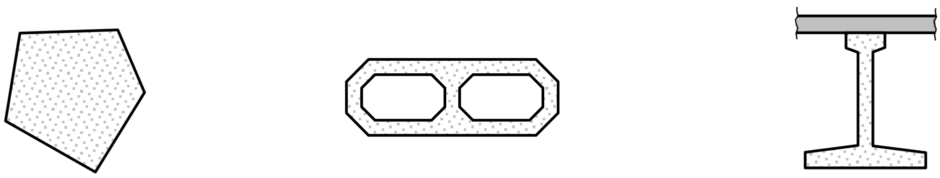

Solid cross-section of arbitrary shape	*Cross-section with holes thick- and thin-walled*	*cross-section composed of several materials*

Fig. 6.3: A general theory is required to analyse cross-sections that are common in the engineering practice.

The approach to be followed is summarised in Fig. 6.4. By definition, the torsional moment M_t is equal to the product of GI_t and the specific torsion θ. However, M_t is also equal to the integral over the cross-sectional area of the shear stress σ times the arm r. This means that a recipe can be formulated for the calculation of GI_t, provided that a value of θ is adopted. For this assumed deformation the stresses σ are determined. The torsional moment in the cross-section then can be obtained by calculation of the integral for $r\sigma$. Because the torsional stiffness GI_t is equal to the torque M_t for $\theta = 1$, the torsional moment of inertia is known too (see Fig. 6.4). Since the stress distribution is known, the largest stress and its position in the cross-section are fixed as well.

RECIPE for the calculation of GI_t
- *find σ for given θ*
- *determine GI_t from*: $GI_t = \dfrac{1}{\theta}\iint\limits_A r\sigma\, dA$

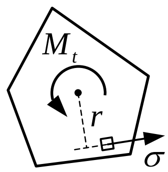

$$\left.\begin{aligned} M_t &= GI_t\theta \\ M_t &= \iint\limits_A r\sigma\, dA \end{aligned}\right\} \rightarrow \quad GI_t\theta = \iint\limits_A r\sigma\, dA$$

Fig. 6.4: The calculation of the torsional stiffness is formulated as a stress problem for an imposed deformation θ.

6.2 Basic equations and boundary conditions

De Saint-Venant has published the theory for torsion in 1855. This theory is correct if at the ends of the bar certain conditions are satisfied. These conditions prescribe that the torsional moments have to be applied via a certain distribution of shear stresses over the cross-section, and that no normal stresses are generated in axial direction at the ends (a dynamic boundary condition). This last condition implies that an eventual distribution of displacements in axial direction can be generated without restrictions, because at the surface where the (surface) load has been prescribed, no kinematic boundary condition can be imposed at the same time.
The right-handed coordinate system is chosen such that the x-direction is parallel to or coincides with the bar axis. So, the y-axis and z-axis are situated in the cross-section (see Fig. 6.5). The figures are drawn in such a manner that the x-axis is pointing backwards. In a

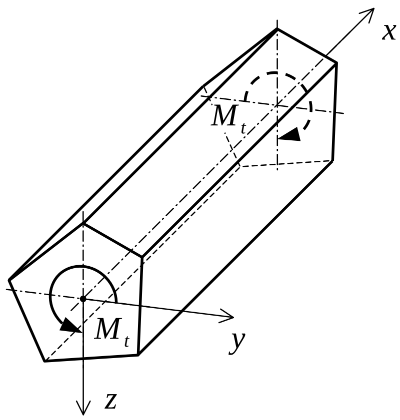

Fig. 6.5: Choice of coordinate system.

three-dimensional stress state, normally three displacements are generated, and in the three corresponding directions a volume load may be applied. Generally, six different stresses with six corresponding strains are present as well. The kinematic, constitutive and equilibrium equations are already provided in chapter 5. Using the brief notation for differentiation, they can be summarised as follows:

Kinematic equations

$$\begin{aligned}
\varepsilon_{xx} &= u_{x,x} \quad ; \quad \gamma_{yz} = u_{y,z} + u_{z,y} \\
\varepsilon_{yy} &= u_{y,y} \quad ; \quad \gamma_{zx} = u_{z,x} + u_{x,z} \\
\varepsilon_{zz} &= u_{z,z} \quad ; \quad \gamma_{xy} = u_{x,y} + u_{y,x}
\end{aligned} \tag{6.1}$$

Constitutive equations

$$\begin{Bmatrix} \sigma_{xx} \\ \sigma_{yy} \\ \sigma_{zz} \end{Bmatrix} = \frac{(1-\upsilon)E}{(1+\upsilon)(1-2\upsilon)} \begin{bmatrix} 1 & \frac{\upsilon}{1-\upsilon} & \frac{\upsilon}{1-\upsilon} \\ & 1 & \frac{\upsilon}{1-\upsilon} \\ \text{symm.} & & 1 \end{bmatrix} \begin{Bmatrix} \varepsilon_{xx} \\ \varepsilon_{yy} \\ \varepsilon_{zz} \end{Bmatrix} \quad ; \quad \begin{Bmatrix} \sigma_{yz} \\ \sigma_{zx} \\ \sigma_{xy} \end{Bmatrix} = G \begin{bmatrix} 1 & 0 & 0 \\ & 1 & 0 \\ \text{symm.} & & 1 \end{bmatrix} \begin{Bmatrix} \gamma_{yz} \\ \gamma_{zx} \\ \gamma_{xy} \end{Bmatrix} \tag{6.2}$$

Equilibrium equations

$$
\begin{aligned}
&\sigma_{xx,x} + \sigma_{yx,y} + \sigma_{zx,z} + P_x = 0 \\
&\sigma_{xy,x} + \sigma_{yy,y} + \sigma_{zy,z} + P_y = 0 \\
&\sigma_{xz,x} + \sigma_{yz,y} + \sigma_{zz,z} + P_z = 0
\end{aligned}
\qquad (6.3)
$$

In the case of torsion the volume forces P_x, P_y and P_z are absent.

Distribution of displacements and stresses

De Saint-Venant succeeded to indicate a displacement field with enough freedom to allow for displacements at the ends, and from which a stress field follows that satisfies all requirements for equilibrium in the volume, along the circumference and at the ends of the bar. In the theory of elasticity only one unique solution can exist, which is in equilibrium with the external load and which satisfies the boundary conditions. Therefore, the solution of De Saint-Venant has to be the correct one.

The displacement field in question will be described now. De Saint-Venant stated that for torsion, the shape of the cross-section is not affected by the deformations. Regarding the displacements u_y and u_z in the plane of the cross-section, the displacement field manifests itself as a rotation about the x-axis as a rigid body.

This rotation is indicated by the symbol φ. This φ is identical to the rotation ω_{yz} as discussed in chapter 5. Further, it can be stated that the displacement u_x can be different from zero and may have a certain distribution over the cross section. However, this distribution is the same for all cross sections. This means that the displacement field is independent of x.

The fact that an arbitrary distribution of u_x can occur over the cross section means that an initially unloaded flat cross-section starts to warp as soon as a torque is applied. Such a displacement field for a bar with square cross-section is drawn in Fig. 6.6. Possible

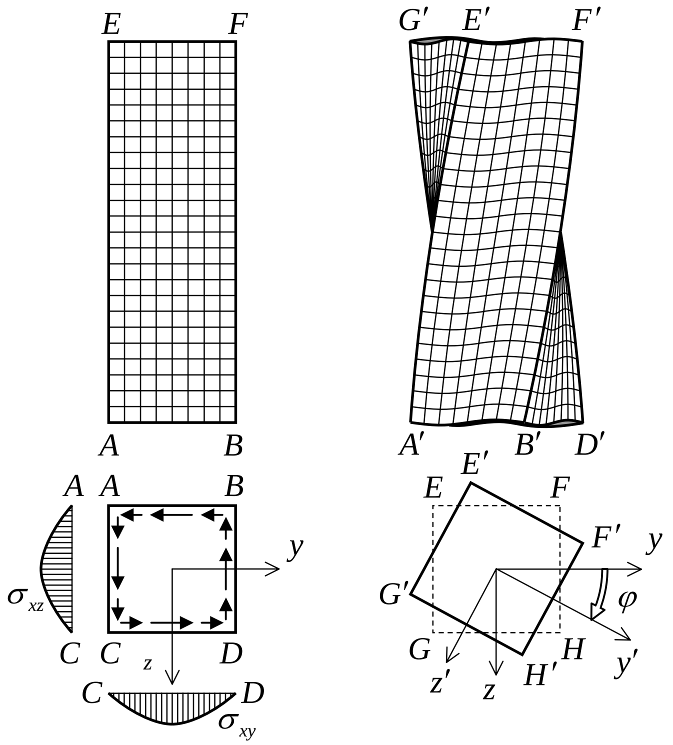

Fig. 6.6: The displacement field is composed of a rotation φ of the cross-section and a warping of the cross-section (the magnitude of φ is very exaggerated).

distributions of the shear stresses have been sketched. Along the edges AC and BD the shear stress σ_{xy} has to be zero. This means that the stress in the points A and B and C and D is zero, but between those points along the edges AB and CD the stress is allowed to increase. The same holds for the shear angle γ_{xy}, which causes the originally rectangular lateral surface $ABEF$ to deform into $A'B'E'F'$ (see Fig. 6.6). The other lateral surfaces experience the same deformation, which makes it plausible that after deformation the originally flat cross-sections are warped.

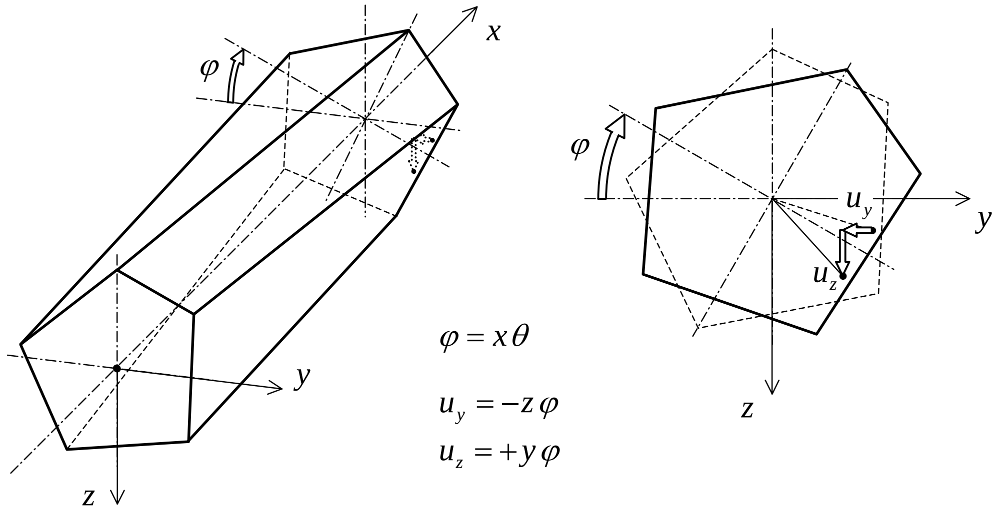

Fig. 6.7: The displacement field described by u_y and u_z.

After this qualitative description of the displacement field, a quantitative formulation will be provided. As a result of the rotation φ, the displacements u_y and u_z in a point x, y, z of the cross-section are equal to (see Fig. 6.7):

$$u_y = -z\,\varphi$$
$$u_z = +y\,\varphi$$

The rotation φ depends on the specific torsion θ. For constant θ, from $d\varphi/dx = \theta$ it follows:

$$\varphi = \theta\, x$$

where it has been used that $\varphi = 0$ for $x = 0$. So, the displacements u_y and u_z become:

$$\begin{aligned} u_y &= -x\,z\,\theta \\ u_z &= +x\,y\,\theta \end{aligned} \qquad (6.4)_a$$

The warping displacement u_x is independent of x, it will increase linearly with the specific torsion θ. Therefore, it can be written:

$$u_x = \psi(y,z)\theta \qquad (6.4)_b$$

where the so-called warping function ψ describes the displacement distribution over the cross-section for $\theta = 1$. In order to check whether this displacement field is suitable for the considered torsion problem, it is substituted into the kinematic equation (6.1). The result is:

$$
\begin{aligned}
&\varepsilon_{xx} = 0 \quad ; \quad && \gamma_{yz} = 0 \\
&\varepsilon_{yy} = 0 \quad ; \quad && \boxed{\gamma_{zx} = \left(\psi_{,z} + y\right)\theta \neq 0} \\
&\varepsilon_{zz} = 0 \quad ; \quad && \boxed{\gamma_{xy} = \left(\psi_{,y} - z\right)\theta \neq 0}
\end{aligned} \tag{6.5}
$$

Only γ_{zx} and γ_{xy} appear to become unequal to zero. Then from the constitutive equations it follows that only the stresses σ_{zx} and σ_{xy} are different from zero too:

$$
\begin{aligned}
&\sigma_{xx} = 0 \quad ; \quad && \sigma_{yz} = 0 \\
&\sigma_{yy} = 0 \quad ; \quad && \boxed{\sigma_{zx} = G\left(\psi_{,z} + y\right)\theta \neq 0} \\
&\sigma_{zz} = 0 \quad ; \quad && \boxed{\sigma_{xy} = G\left(\psi_{,y} - z\right)\theta \neq 0}
\end{aligned} \tag{6.6}
$$

The stresses σ_{zx} and σ_{xy} are the shear stresses in the cross-section that correspond with the torsional moment in the cross-section. So, the chosen displacement field satisfies the requirements. Of the three equilibrium equations (6.3), only the first one is important for the equilibrium of the bar. The second and third one are satisfied automatically, because differentiation of ψ with respect to x yields zero, i.e.:

$$
\begin{aligned}
&0 \; \boxed{+\sigma_{yx,y} + \sigma_{zx,z} = 0} \\
&0 + 0 + 0 = 0 \\
&0 + 0 + 0 = 0
\end{aligned} \tag{6.7}
$$

In Fig. 6.8 it is demonstrated how the remaining equilibrium equation can be interpreted. An elementary cube of material is considered the edges of which have unit length and are parallel to the coordinate directions. In the face coinciding with the cross-section the shear stresses σ_{xy} and σ_{xz} are present. In the x-direction, on the faces with constant y and z, their counterparts σ_{yx} and σ_{zx} can be found. As shown these stresses increase in y and z direction, respectively. The requirement that the cube is in equilibrium in x-direction, directly leads to the obtained equilibrium equation.

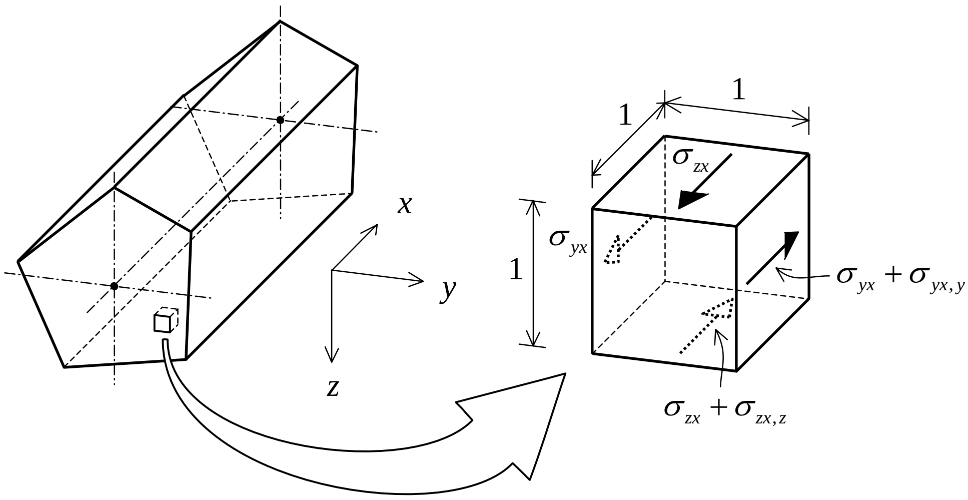

Fig. 6.8: Interpretation of the equilibrium equation in x-direction.

Summarising, for the special case of the De Saint-Venant torque, the general three-dimensional kinematic, constitutive and equilibrium equations reduce to:

$$\boxed{\begin{aligned}\gamma_{zx} &= \left(\psi_{,z} + y\right)\theta \\ \gamma_{xy} &= \left(\psi_{,y} - z\right)\theta\end{aligned}} \qquad (\textit{kinematic equations}) \tag{6.8}$$

$$\boxed{\left.\begin{aligned}\sigma_{zx} &= G\gamma_{zx} \\ \sigma_{xy} &= G\gamma_{xy}\end{aligned}\right\} \Leftrightarrow \left\{\begin{aligned}\gamma_{zx} &= \frac{1}{G}\sigma_{zx} \\ \gamma_{xy} &= \frac{1}{G}\sigma_{xy}\end{aligned}\right.} \qquad (\textit{constitutive equations}) \tag{6.9}$$

$$\boxed{\sigma_{yx,y} + \sigma_{zx,z} = 0} \qquad (\textit{equilibrium equation}) \tag{6.10}$$

The problem contains only one degree of freedom, the warping function $\psi(y,z)$; this corresponds with the fact that just one equilibrium equation is present. No volume load in x-direction exists. Only two stresses and their corresponding strains are different from zero, therefore just two kinematic equations and two constitutive equations remain.
The scheme of relations as depicted in Fig. 6.9 is applicable. The two stresses $\sigma_{xz} = \sigma_{zx}$ and

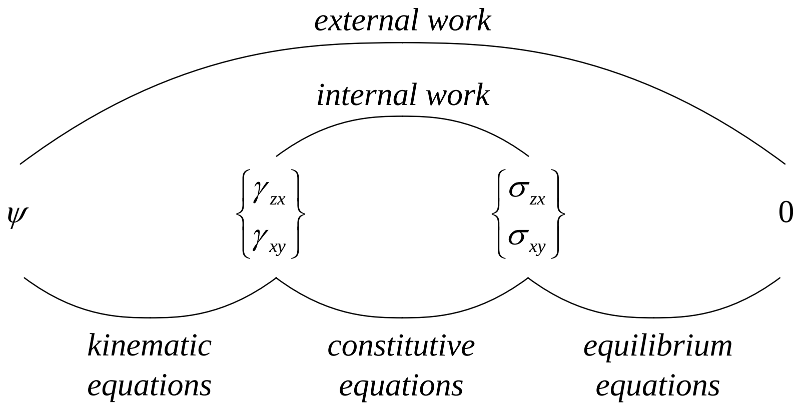

Fig. 6.9: Diagram displaying the relations between the quantities playing a role in the analysis of the De Saint-Venant torsion.

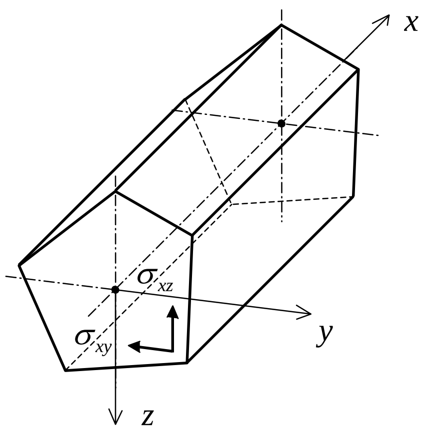

Fig. 6.10: A torsional moment will generate shear stresses σ_{xz} and σ_{xy}.

$\sigma_{xy} = \sigma_{yx}$, which play a role in the assumed displacement field of the problem, are exactly the shear stresses in the cross-section that are caused by the torsional moment. This has been depicted in Fig. 6.10.

Dynamic boundary conditions

The two stresses σ_{xz} and σ_{xy} can also satisfy the dynamic boundary conditions along the circumference of the bar. Generally a normal stress σ_{nn} and two shear stresses σ_{ns} and σ_{nx} are present on the cylindrical surface (see Fig. 6.11). The stresses σ_{nn} and σ_{ns} follow via

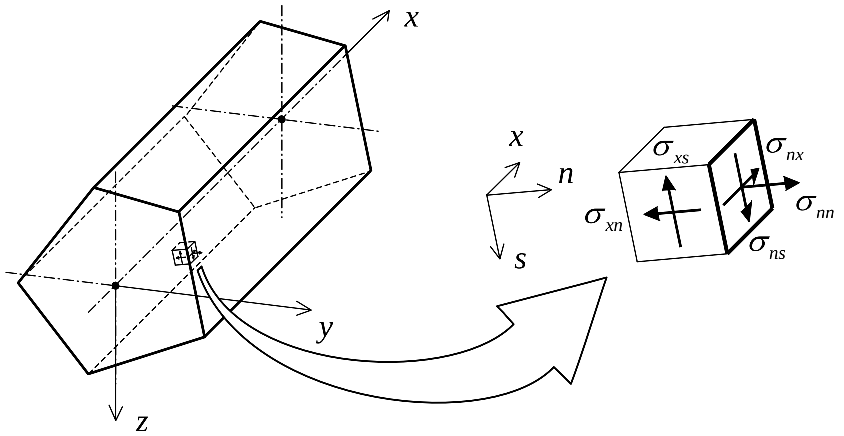

Fig. 6.11: The stresses resulting from the displacement field of De Saint-Venant can satisfy the condition that the stresses σ_{nn}, σ_{ns} and σ_{nx} along the outer surface are zero.

a transformation from the stresses σ_{yy}, σ_{yz} and σ_{zz}. Because all these stresses are zero, the stresses σ_{nn} and σ_{ns} will be zero too. The shear stress σ_{nx} is equal to σ_{xn}, which is situated in the plane of the cross-section. The shear stresses σ_{xn} and σ_{xs} can be obtained via a transformation in the same plane of the shear stresses σ_{xz} and σ_{xy}. The stresses σ_{xs} and σ_{xn} are tangent and normal to the circumference of the cross-section, respectively. The stress σ_{xn} has to be zero, because σ_{nx} cannot occur on the stress-free cylindrical surface. In other words, a completely stress-free cylindrical surface can be realised by requiring that σ_{nx} is zero, i.e.:

$$\boxed{\sigma_{xn} = 0} \qquad (\textit{dynamic boundary condition}) \tag{6.11}$$

Solution strategies

After the formulation of the three sets of basic equations, the next step is the establishment of the solution procedure for these equations. Again the two strategies of the displacement and force method can be followed. Both methods will be discussed and it will become clear that the displacement method leads to a simple and concise formulation for both solid cross-sections and cross-sections with holes. The force method provides a simple formulation only for solid cross-sections, for cross-sections with holes the formulation becomes rather complicated. Nevertheless, in the past the force method was used in the classical approach of the torsional problem. The reason was that for this method a number of analogies exist that provided a lot of insight into the problem. Nowadays in the computer age, no clear preference for one of the methods exists and both methods can be applied. However, in this course most of the attention is paid to the force method, because this method links up with the visual imagination of the engineer.

6.3 Displacement method

Differential equation
In the procedure of the displacement method, successive substitutions take place from the kinematic equations towards the equilibrium equation. Here the constitutive equations are used in stiffness formulation. Doing so, the equilibrium equation is transformed into a differential equation for the unknown degree of freedom ψ. The procedure can be summarised by:

$$\left.\begin{aligned} \gamma_{zx} &= \left(\psi_{,z} + y\right)\theta \\ \gamma_{xy} &= \left(\psi_{,y} - z\right)\theta \end{aligned}\right\} \quad (\textit{kinematic equations})$$

$$\left.\begin{aligned} \sigma_{zx} &= G\gamma_{zx} \\ \sigma_{xy} &= G\gamma_{xy} \end{aligned}\right\} \quad (\textit{constitutive equations})$$

$$\sigma_{yx,y} + \sigma_{zx,z} = 0 \quad (\textit{equilibrium equation})$$

$$\boxed{G\left(\psi_{,yy} + \psi_{,zz}\right)\theta = 0} \qquad (6.12)$$

Because G and θ are constants, the found differential equation simply states that the Laplace operator of ψ is equal to zero:

$$\boxed{\psi_{,yy} + \psi_{,zz} = 0} \qquad (6.13)$$

Boundary condition
For the solution of differential equation (6.13) it is required to reformulate the boundary condition $\sigma_{xn} = 0$ in terms of ψ. This can be done as follows.
The condition $\sigma_{xn} = 0$ implies that the deformation $\gamma_{xn} = 0$ too. For this deformation it can be written:

$$\gamma_{xn} = u_{x,n} + u_{n,x}$$

The displacement u_n can simply be expressed in u_y and u_z by the following transformation formula (also see Fig. 6.12):

$$u_n = u_y \cos\alpha + u_z \sin\alpha$$

The expression for the deformation becomes:

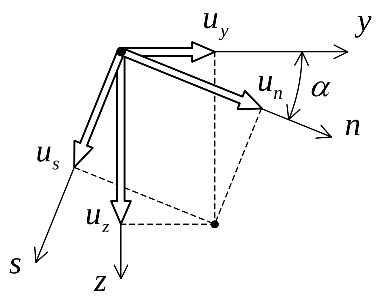

$$u_n = +u_y \cos\alpha + u_z \sin\alpha$$
$$u_s = -u_y \sin\alpha + u_z \cos\alpha$$

Fig. 6.12: Transformation of displacements in the plane of the cross-section.

$$\gamma_{xn} = u_{x,n} + u_{y,x}\cos\alpha + u_{z,x}\sin\alpha$$

Finally, the relations for u_x, u_y and u_z given by (6.4) are substituted, they read:

$$u_x = \psi\theta \quad ; \quad u_y = -xz\theta \quad ; \quad u_z = xy\theta$$

The requirement that γ_{xn} is zero delivers the relation:

$$\left(\psi_{,n} - z\cos\alpha + y\sin\alpha\right)\theta = 0$$

or differently written, it delivers the condition for the slope of ψ perpendicular to the edge:

$$\boxed{\psi_{,n} = z\cos\alpha - y\sin\alpha} \qquad (6.14)$$

In each point of the edge the values of y, z and α are known, so that $\psi_{,n}$ is prescribed along the entire circumference. The solution of differential equation (6.13) together with boundary condition (6.14) is classified as a problem of the *Neumann type*. Now from a mathematical point of view, the warping function ψ is determined and can be solved. After that γ_{zx} and γ_{xy} can be solved from the kinematic equations, which also determine the values of the stresses. For obtaining a correct solution for ψ, in one point of the cross-section a value of ψ has to be prescribed in order to prevent a rigid body movement of the body in x-direction.

Hollow Cross-sections

When the cross-section is not solid but contains one or more holes, the procedure is not essentially more difficult. Then along the circumference of each hole the dynamic boundary condition $\sigma_{xn} = 0$ applies too. This means that along the holes the condition (6.14) for $\psi_{,n}$ has to be imposed.

6.4 Force method

In the force method a solution for the stresses is sought that a priori satisfies the equilibrium equations and dynamic boundary conditions. Because one equilibrium equation exists for the two unknown stresses σ_{xy} and σ_{xz}, the problem is statically indeterminate to the first degree.

Therefore, only one stress function has to be introduced, which just like the stresses is a function of y and z. In this case, a stress function that meets the conditions is defined by:

$$\sigma_{xy} = \phi_{,z} \quad ; \quad \sigma_{xz} = -\phi_{,y} \tag{6.15}$$

These relations between the stresses and the redundant ϕ guarantee that the equilibrium equation $\sigma_{yx,y} + \sigma_{zx,z} = 0$ is satisfied automatically. For the determination of ϕ a compatibility condition has to be formulated. This condition is found by elimination of the degree of freedom ψ from the two kinematic equations:

$$\gamma_{zx} = \left(\psi_{,z} + y\right)\theta \quad ; \quad \gamma_{xy} = \left(\psi_{,y} - z\right)\theta$$

When both equations are differentiated with respect to y and z respectively, the two equations contain the term $\psi_{,yz}$, which easily can be eliminated. The result reads:

$$\gamma_{xz,y} - \gamma_{xy,z} = 2\theta \tag{6.16}$$

where $\gamma_{zx,y}$ is replaced by $\gamma_{xz,y}$. It appears that the deformations γ_{xz} and γ_{xy} cannot obtain independently any value, they are coupled.

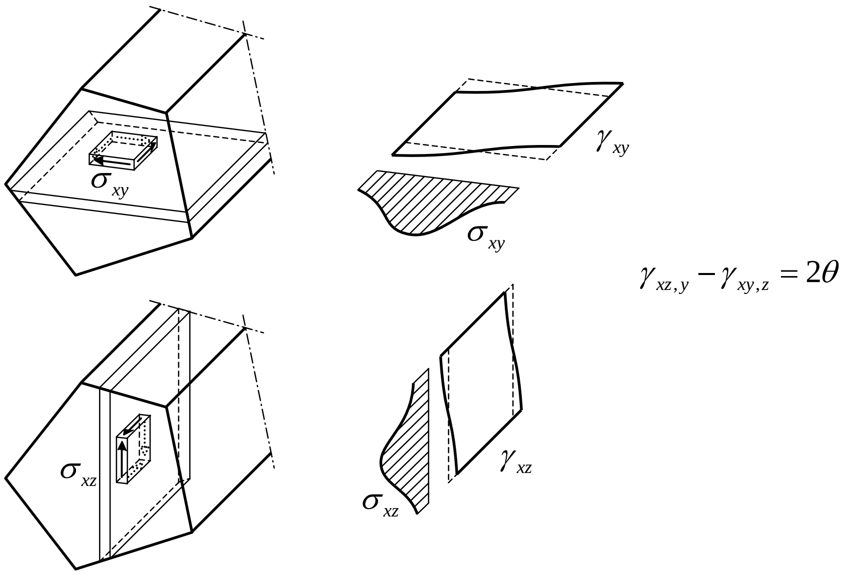

Fig. 6.13: The deformations γ_{xy} and γ_{xz} have to be compatible.

On basis of Fig. 6.13, a physical interpretation of the compatibility condition can be given. In a horizontal slice of the bar the shear stresses σ_{xy} generate the shear angles γ_{xy}. The originally rectangular slice deforms into another shape. At the same time a vertical rectangular slice deforms under the influence of the shear stresses σ_{xz}, which initiate the shear angles γ_{xz}. All those horizontal and vertical slices have to fit precisely during deformation, such that a continuous warped cross-section is maintained. This means that there has to be a relation between the deformations γ_{xy} and γ_{xz}.
The solution strategy now is the successive substitution from the equilibrium equation up to the compatibility equation. In this case, the constitutive equations are given in flexibility formulation, i.e.:

$$\boxed{-\frac{1}{G}\left(\phi_{,yy}+\phi_{,zz}\right)=2\theta} \qquad (6.17)$$

$$\gamma_{xz,y}-\gamma_{xy,z}=2\theta \qquad (\textit{compatibility equation})$$

$$\left.\begin{aligned}\gamma_{xy}&=\frac{1}{G}\sigma_{xy}\\ \gamma_{xz}&=\frac{1}{G}\sigma_{xz}\end{aligned}\right. \qquad (\textit{constitutive equations})$$

$$\left.\begin{aligned}\sigma_{xy}&=+\phi_{,z}\\ \sigma_{xz}&=-\phi_{,y}\end{aligned}\right. \qquad (\textit{equilibrium equations})$$

It can be seen that the force method results in a Laplace equation too. However, in this case the right-hand side is not equal to zero.

Remark
In (6.15) the stress function is defined in such a manner that the stress σ_{xy}, which is acting in y-direction is equal to the derivative of ϕ in the z-direction perpendicular to that. Likewise, the value of the stress σ_{xz} is equal to the derivative of ϕ in perpendicular direction (except for the sign). It can be shown that this property also holds for the shear stresses σ_{xn} and σ_{xs} in arbitrarily chosen orthogonal directions n and s (see Fig. 6.14):

$$\sigma_{xn}=+\phi_{,s} \quad ; \quad \sigma_{xs}=-\phi_{,n} \qquad (6.18)$$

To prove this, the stresses σ_{xn} and σ_{xs} and also $\phi_{,n}$ and $\phi_{,s}$ will be expressed in $\phi_{,y}$ and $\phi_{,z}$. From the results, relation (6.18) can be confirmed.
Fig. 6.14 shows that the coordinates and the shear stresses in the cross-section transform by the same rule. In the expression for the stresses, σ_{xy} and σ_{xz} are replaced by respectively $\phi_{,z}$ and $-\phi_{,y}$. This results in:

$$\begin{aligned}\sigma_{xn}&=+\phi_{,z}\cos\alpha-\phi_{,y}\sin\alpha\\ \sigma_{xs}&=-\phi_{,z}\sin\alpha+\phi_{,y}\cos\alpha\end{aligned} \qquad (6.19)$$

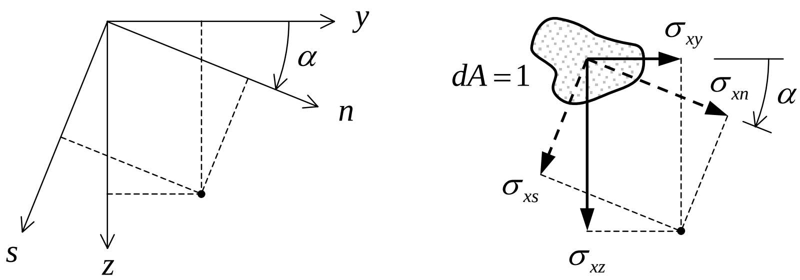

$$\begin{aligned}n&=+y\cos\alpha+z\sin\alpha\\ s&=-y\sin\alpha+z\cos\alpha\end{aligned} \qquad \begin{aligned}\sigma_{xn}&=+\sigma_{xy}\cos\alpha+\sigma_{xz}\sin\alpha\\ \sigma_{xs}&=-\sigma_{xy}\sin\alpha+\sigma_{xz}\cos\alpha\end{aligned}$$

Fig. 6.14: Transformation of coordinates and shear stresses in the cross-section.

By using the chain rule, $\phi_{,n}$ and $\phi_{,s}$ can be expressed in $\phi_{,y}$ and $\phi_{,z}$:

$$\phi_{,n} = \phi_{,y}\, y_{,n} + \phi_{,z}\, z_{,n}$$
$$\phi_{,s} = \phi_{,y}\, y_{,s} + \phi_{,z}\, z_{,s}$$

To determine the derivatives of y and z with respect to n and s, the coordinate transformations of Fig. 6.14 are inverted:

$$y = n\cos\alpha - s\sin\alpha$$
$$z = n\sin\alpha + s\cos\alpha$$

This leads to the expressions:

$$\begin{aligned} \phi_{,n} &= +\phi_{,y}\cos\alpha + \phi_{,z}\sin\alpha \\ \phi_{,s} &= -\phi_{,y}\sin\alpha + \phi_{,z}\cos\alpha \end{aligned} \tag{6.20}$$

Comparison of (6.19) with (6.20) shows that relation (6.18) is generally valid.

Boundary conditions

The dynamic boundary condition along the circumference of a solid cross-section reads:

$$\sigma_{xn} = 0$$

where n is normal to the edge and pointing outward (see Fig. 6.15). On basis of (6.18) it then follows that:

$$\phi_{,s} = 0$$

The derivative in the direction of the circumference is equal to zero. This means that ϕ has a constant value along the circumference. For a solid section this constant value can be set to zero without any loss of general validity, for the stresses are obtained by differentiation of ϕ so that the constant disappears. Therefore, as boundary condition it will be prescribed:

$$\phi = 0 \tag{6.21}$$

The found differential equation and corresponding boundary condition given by:

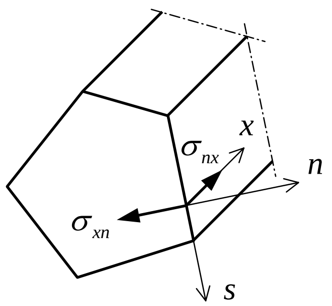

$$\boxed{\begin{array}{c} \sigma_{xn} = 0 \quad \rightarrow \quad \phi_{,s} = 0 \quad \rightarrow \\ \phi = \text{ constant} \quad \rightarrow \quad \text{choose } \phi = 0 \end{array}}$$

Fig. 6.15: Boundary condition along the circumference of the bar.

$$\boxed{\begin{array}{l} -\dfrac{1}{G}\left(\phi_{,yy}+\phi_{,zz}\right)=2\theta \\ \phi=0 \end{array}} \qquad \begin{array}{l} (\textit{differential equation}) \\ (\textit{boundary condition}) \end{array} \tag{6.22}$$

determine in mathematical sense the torsional problem in the force method. In this way the problem is written in the so-called Dirichlet formulation. The stress function ϕ can be solved from the set (6.22), after which the stresses can be found by the derivatives of the function ϕ:

$$\boxed{\begin{array}{l} \sigma_{xy}=+\phi_{,z} \\ \sigma_{xz}=-\phi_{,y} \end{array}} \tag{6.23}$$

The ϕ-bubble

From the simple torsional problem of the circular cross-section, as discussed in previous courses, it is known that the shear stresses are zero in the centre of the cross-section and that the "round-going" stresses increase in radial direction. This pattern can be expected for cross-sections of arbitrary shape too. In the point where the stresses σ_{xy} and σ_{xz} are zero, the derivatives $\phi_{,z}$ and $\phi_{,y}$ have to be zero. At that position the function ϕ obtains an extreme value, while ϕ is zero on the edge. When a section is made through the distribution of ϕ perpendicular to the cross-section a sort of hood covering of the cross-section can be noticed, which will be called the "ϕ-bubble" (see Fig. 6.16). The slopes of the ϕ-bubble determine the magnitude of the stresses. Indeed it can be observed that the stresses increase towards the edge.

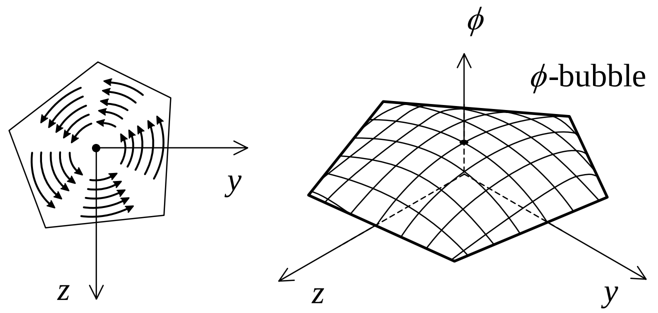

on circumference $\rightarrow \quad \phi = 0$

in point where $\left.\begin{array}{l}\phi_{,y}=0\\ \phi_{,z}=0\end{array}\right\} \rightarrow \quad \phi=\phi_{\max}$

Fig. 6.16: The distribution of ϕ over the cross-section is called a "ϕ-bubble".

Check of the shear forces

It was shown that σ_{xy} and σ_{xz} are the only stresses present, and how they can be determined. In general, the resultants of these stresses over the cross-section may be a torsional moment M_t and the shear forces V_y and V_z. In the case of torsion, the stress distribution should be statically equivalent with a torsional moment M_t, while the shear forces V_y and V_z are zero. Therefore, the values of the shear forces will be checked.
The horizontal shear force equals:

$$V_y = \iint_A \sigma_{xy}\, dA = \iint_A \frac{\partial\phi}{\partial z} dy dz$$

First, integration is carried out in z -direction and then in y -direction (see Fig. 6.17):

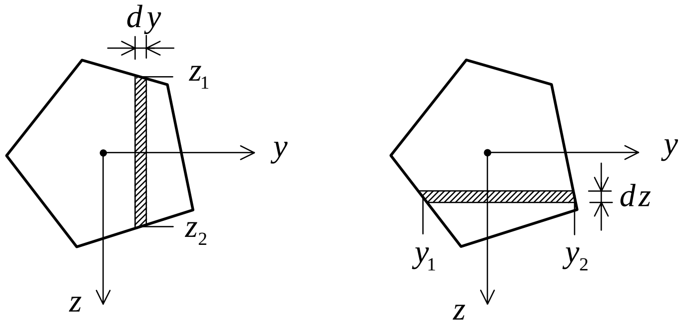

for calculation of V_y *for calculation of V_z*

Fig. 6.17: Integration paths required for the conformation that V_y and V_z are zero.

$$V_y = \int \left\{ \int_{z_1}^{z_2} \frac{\partial\phi}{\partial z} dz \right\} dy = \int \left\{ \int_{z_1}^{z_2} d\phi \right\} dy = \int \left(\phi_2 - \phi_1\right) dy = 0$$

At the edge the values of ϕ_1 and ϕ_2 are both zero, which means that V_y is zero too.
For the vertical shear force a similar approach is adopted. In this case the integration is first carried out in y -direction:

$$V_z = -\iint_A \sigma_{xz}\, dA = -\iint_A \frac{\partial\phi}{\partial y} dy dz \quad \rightarrow \quad V_z = -\int \left\{ \int_{y_1}^{y_2} d\phi \right\} dz = -\int \left(\phi_2 - \phi_1\right) dz = 0$$

The resulting torsional moment
During the problem definition in section 6.1, the resulting moment was written as:

$$M_t = \iint_A r\, \sigma\, dA$$

This integral can be worked out into more detail by introducing the shear stresses σ_{xy} and σ_{xz} with their arms z and y, respectively. As can be observed in Fig. 6.18, positive values of σ_{xy} deliver moments that reduce the torque and the positive values of σ_{xz} increase the torque (in the first quadrant). Therefore, the expression of the torsional moment becomes:

$$M_t = \iint \left(y\, \sigma_{xz} - z\, \sigma_{xy} \right) dA \qquad (6.24)$$

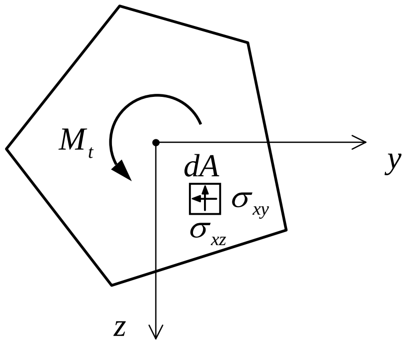

Fig. 6.18: Calculation of the resulting torsional moment.

It is advantageous to solve integral (6.24) in two parts. During the solution process integration by parts takes place. It is recalled to mind how this is done. Two functions $u(x)$ and $v(x)$ are considered on the interval $x_1 \le x \le x_2$. For x_1 the function values are u_1 and v_1 and for x_2 they are u_2 and v_2. For the product of the two functions it holds:

$$\int_{x_1}^{x_2} d(u\,v) = u_2 v_2 - u_1 v_1 \quad \text{or} \quad \int_{x_1}^{x_2} u\,dv + \int_{x_1}^{x_2} v\,du = u_2 v_2 - u_1 v_1$$

As rule for integration by parts, the last expression is used in the form:

$$\int_{x_1}^{x_2} u\,dv = -\int_{x_1}^{x_2} v\,du + \left(u_2 v_2 - u_1 v_1\right) \tag{6.25}$$

After this short intermezzo, it is continued with the determination of the surface integral of the vertical stresses. They deliver a share in the torsional moment given by:

$$M_{vertical} = \iint_A y\,\sigma_{xz}\,dA = \iint_A -y\frac{\partial\phi}{\partial y}\,dy\,dz$$

First the integration in y-direction is performed, see Fig. 6.19:

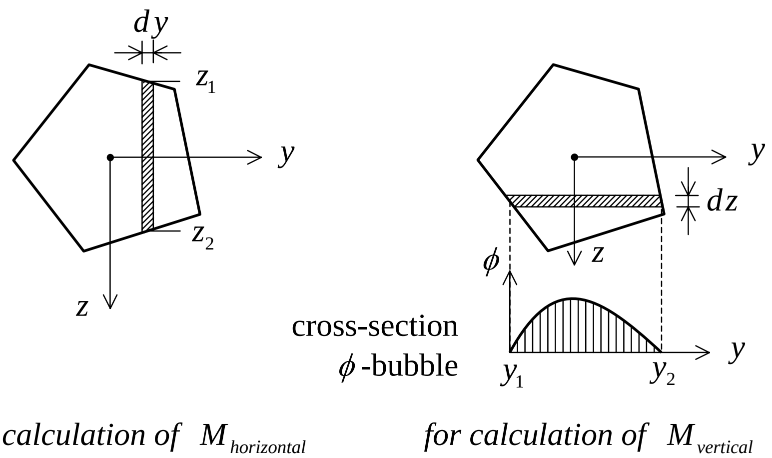

for calculation of $M_{horizontal}$ *for calculation of* $M_{vertical}$

Fig. 6.19: Integration paths for the calculation of $M_{vertical}$ *and* $M_{horizontal}$.

$$M_{vetical} = \int \left(\int_{y_1}^{y_2} -y \frac{\partial \phi}{\partial y}\, dy \right) dz = \int \left(\int_{y_1}^{y_2} -y\, d\phi \right) dz$$

Now, the integral in y-direction will be integrated by parts according to the rule (6.25). Then it is found:

$$-\int_{y_1}^{y_2} y\, d\phi = \int_{y_1}^{y_2} \phi\, dy - \left(y_2\, \phi_2 - y_1\, \phi_1 \right)$$

Because ϕ_1 and ϕ_2 are situated on the edge they are zero, so that the following remains:

$$\int_{y_1}^{y_2} \phi\, dy \qquad (\textit{area of the vertical section of the } \phi\textit{-bubble}) \tag{6.26}$$

This result is exactly the area of the considered vertical section of the ϕ-bubble. It then is clear that the moment of the vertical stresses is equal to the volume of the ϕ-bubble:

$$\boxed{M_{vertical} = \iint_A \phi\, dy dz} \qquad (\textit{volume of the } \phi\textit{-bubble}) \tag{6.27}$$

In an analogous manner the contribution of $M_{horizontal}$ is calculated. For that purpose integration in z-direction is carried out. Also for this case it is found:

$$\boxed{M_{horizontal} = \iint_A \phi\, dy dz} \qquad (\textit{volume of the } \phi\textit{-bubble}) \tag{6.28}$$

Therefore, the total result for the torsional moment becomes:

$$\boxed{M_t = 2 \iint_A \phi\, dA} \qquad (\textit{two times the volume of the } \phi\textit{-bubble}) \tag{6.29}$$

Recalling to mind that for this moment it also holds $M_t = GI_t \theta$, for the torsional stiffness it is found:

$$\boxed{GI_t = \frac{2}{\theta} \iint_A \phi\, dA} \tag{6.30}$$

Conclusions

Up to now, results have been derived which are worthwhile mentioning in a summary. Fig. 6.20 supports these conclusions.

- The stiffness GI_t and the torsional moment M_t are determined by the double volume of the ϕ-bubble (for $\theta = 1$).
- The shear stress is determined by the slope of the ϕ-bubble perpendicular to the direction of the stress. This property holds for every direction.
- It appears that the contribution of the vertical and horizontal stresses to GI_t and M_t is the same, namely one volume of the ϕ-bubble each. This generally holds irrespective the shape of the cross-section, for example for a strip-shaped as well as a square cross-section.

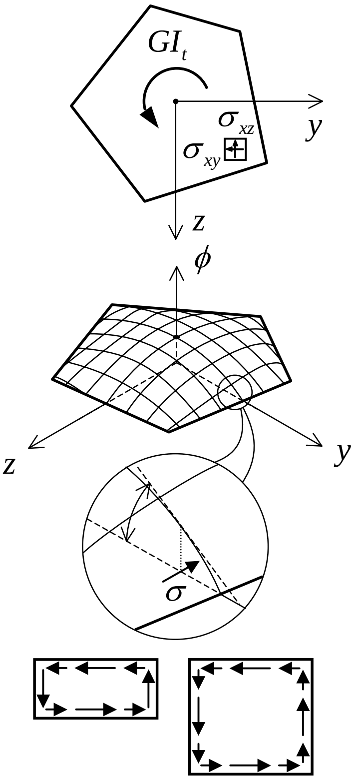

CONCLUSIONS

- Stiffness = 2 times volume of ϕ-bubble for $\theta = 1$
- Shear stress = slope of the ϕ-bubble
- The contributions of $\sigma_{vertical}$ and $\sigma_{horizontal}$ are equal

Fig. 6.20: Summary of the conclusions.

Remarks

1. The x-axis has been chosen arbitrarily parallel to the bar axis. The displacement field (6.4) contains a rotation about the x-axis. This creates the impression that this axis has certain special properties. However, this is not the case, because an extra rotation as a rigid body about the y- and z-axes can be added to the displacement field (6.4), such that any other line parallel to the x-axis start to act as the rotation axis. For the displacement field it then has to be chosen:

$$u_x = \psi(y,z)\theta - by\theta + az\theta$$

rotation about y-axis

$$u_y = x\left(z-b\right)\theta$$

rotation about z-axis

$$u_z = x\left(y-a\right)\theta$$

It simply can be established that the additional terms have no influence on the stresses, and that now the rotation takes place about the axis $y = a, z = b$. So, this indicates that the x-axis indeed can be chosen arbitrarily without loss of generality provided that it is parallel to the axis of the bar.

2. During the analysis it was made clear that σ_{xx} has to be zero, also at the ends of the bar and that for that reason the warping cannot be prevented. In section 6.12 the consequences of a prevented warping will be discussed. Theoretically, the shear stresses σ_{xy} and σ_{xz} at the ends have to be distributed exactly as the derivatives of the stress function ϕ prescribe. If this is not the case at the ends an interference length will occur in which the stress-state gradually evolves to the distribution according to the derivatives of ϕ.

3. The surface integral for M_t given by (6.29) could have been determined directly from (6.24) by replacement of σ_{xy} and σ_{xz} by the respective derivatives of ϕ, which is followed by the application of the proposition of Green for the transformation of a surface integral into a contour integral. However, the disadvantage of this approach is that it would not have revealed that the contributions of the horizontal and vertical stresses to the moment are identical.

6.5 Exact solution for an elliptic cross-section

For some cross-sections, it appears to be possible to derive an exact solution for the differential equation and boundary condition (6.22). An example is the elliptic cross-section (see Fig. 6.21). The equation of the edge in this case is:

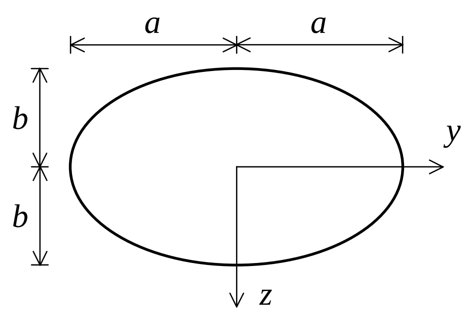

Fig. 6.21: Elliptic cross-section.

$$\frac{y^2}{a^2} + \frac{z^2}{b^2} = 1$$

Then the following function is zero all along the edge:

$$A\left(1 - \frac{y^2}{a^2} - \frac{z^2}{b^2}\right)$$

It turns out that the differential equation can be satisfied if ϕ is made equal to this function:

$$\phi = A\left(1-\frac{y^2}{a^2}-\frac{z^2}{b^2}\right)$$

Substitution of this relation into differential equation (6.22) yields the following result for A:

$$A = G\frac{a^2b^2}{a^2+b^2}\theta$$

Therefore, the solution is:

$$\boxed{\phi = G\frac{a^2b^2}{a^2+b^2}\left(1-\frac{y^2}{a^2}-\frac{z^2}{b^2}\right)\theta} \tag{6.31}$$

Using (6.15) the shear stresses become:

$$\sigma_{xy} = -2G\frac{a^2z}{a^2+b^2}\theta \quad ; \quad \sigma_{xz} = +2G\frac{b^2y}{a^2+b^2}\theta \tag{6.32}$$

The shear stresses are linearly distributed along straight lines through the origin, just as known for the circular cross-section (see Fig. 6.22). The largest shear stress occurs on the edge at the short axis (at $y=0$, $z=\pm b$, when $a>b$). The absolute value of this stress is:

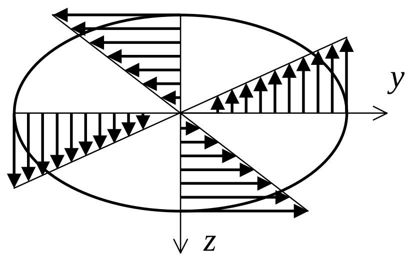

In this figure the x-axis is pointing into the paper

Fig. 6.22: Stress distribution in an elliptic cross-section.

$$\sigma_{\max} = 2G\frac{a^2b}{a^2+b^2}\theta \quad \text{for} \quad a>b$$

The torsional moment is according to (6.29) two times the volume of the ϕ-bubble:

$$M_t = 2G\frac{a^2b^2}{a^2+b^2}\left\{\iint dy\,dz - \frac{1}{a^2}\iint y^2dy\,dz - \frac{1}{b^2}\iint z^2dy\,dz\right\}\theta$$

The first integral is the area of the ellipse, πab. The second and third integrals are the moments of inertia with respect to the z-axis and y-axis, respectively. The values are equal to $\pi a^3b/4$ and $\pi ab^3/4$, respectively. Thus the term between braces equals $\pi ab/2$ and the moment becomes:

$$M_t = G\pi \frac{a^3 b^3}{a^2 + b^2}\theta \tag{6.33}$$

Because it also holds:

$$M_t = G I_t \theta$$

For an ellipse it apparently is found:

$$I_t = \frac{\pi a^3 b^3}{a^2 + b^2} \tag{6.34}$$

By using (6.33), the relations (6.32) for the stresses can be expressed in the torsional moment M_t:

$$\sigma_{xy} = -\frac{z\, M_t}{\frac{1}{2}\pi a b^3} \quad ; \quad \sigma_{xz} = +\frac{y\, M_t}{\frac{1}{2}\pi a^3 b} \tag{6.35}$$

A designer mainly will be interested in the maximum shear stress. Expressed in the torsional moment this shear stress equals:

$$\sigma_{\max} = \frac{M_t}{\frac{1}{2}\pi a b^2} \quad \text{for} \quad a > b \tag{6.36}$$

6.6 Membrane analogy

Already during the discussion of the force method it was mentioned that analogies can be used. *Prandtl* introduced a well-known analogy. He recognised that the differential equation for the torsional problem was similar to the problem of a membrane under tension. This so-called *membrane analogy* is depicted in Fig. 6.23.

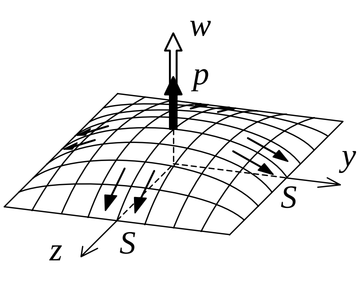

ANALOGY

- shape of membrane = shape of cross-section
- $p = 2\theta$
- $s = 1/G$

$$-S\left(w_{,yy} + w_{,zz}\right) = p$$

on edge: $w = 0$

$$-\frac{1}{G}\left(\phi_{,yy} + \phi_{,zz}\right) = 2\theta$$

on edge: $\phi = 0$

Fig. 6.23: The differential equations for a stressed membrane and for torsion have the same character.

The bending stiffness of the membrane is very low. In the plane of the membrane an omnidirectional tensile force per unit of width is present. When a part of the membrane is considered with unit width in z-direction and length dy, it can be modelled as a cable. For

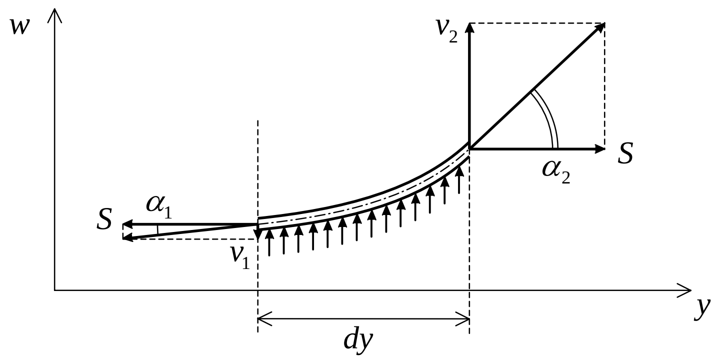

Fig. 6.24: Free-body diagram.

sufficiently small deflection w under a constant excess pressure p, the vertical equilibrium of this part of the membrane equals (see Fig. 6.24):

$$v_1 - v_2 = p\,dy$$

where v_1 and v_2 are the membrane shear forces, for which it can be written:

$$v_1 = S\,\alpha_1 \quad ; \quad v_2 = S\,\alpha_2$$

So:

$$S\left(\alpha_1 - \alpha_2\right) = p\,dy$$

Further, for the increase of the slope it holds:

$$\alpha_2 - \alpha_1 = w_{,yy}dy$$

This provides:

$$-S\,w_{,yy}\,dy = p\,dy \quad \rightarrow \quad -S\,w_{,yy} = p$$

When both the y-direction and z-direction are considered, the differential equation for a membrane is found:

$$\boxed{-S\left(w_{,yy} + w_{,zz}\right) = p} \tag{6.37}$$

Experimental membrane analogy

The membrane analogy can be utilised experimentally as discussed below. A box is made with vertical walls and horizontal bottom. The horizontal top of the box is open and is covered by a stretched rubber membrane. The plan view of the box has the shape of the cross-section to be investigated. By pressurising the inside of the box, the membrane will bulge out. A shape will be created similar to the ϕ-bubble (Fig. 6.23 shows this phenomenon for a rectangular cross-section). By measurement of the slope of the membrane in different points, the stress distribution over the cross-section can be determined. In literature articles can be found of how this was done in the past with *soap films*. Therefore, this approach is also called the *soap-film analogy*.

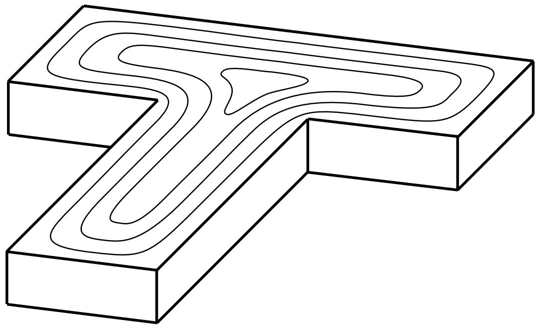

Fig. 6.25: Example of contour lines for a T-shaped cross-section.

A method to visualise the membrane surface is the drawing of contour lines of constant ϕ (see Fig. 6.25). When a s-n coordinate system is attached with s parallel and n perpendicular to the contour line, then along the contour line it holds $w_{,s} = 0$ and therefore $\phi_{,s} = 0$. This means that σ_{xn} is zero and only the shear stress σ_{xs} is present. So, the direction of the shear stress is tangent to the contour lines. The contour lines can be drawn at constant intervals of w (and thus ϕ). Then it can be concluded that the shear stress σ_{xs} is large where the density of he contour lines is high, because at those spots the gradient $\phi_{,n}$ is large. The contour lines can be visualised by the so-called “shadow moiré”. With optical means, the lines of constant displacement are visualised, with a constant difference in displacement between the lines.

Membrane analogy as mental experiment
The membrane analogy can be used too, without the actual execution of a real test with a membrane. The analogy is applied as a mental experiment. This can be done both qualitatively and quantitatively. Qualitatively, the analogy is useful, since it provides an indication where the largest shear stresses will occur and how the cross-section can be adapted to optimise it for torsion. Fig. 6.26 shows a triangular cross-section. When a soap film is imagined under pressure over this cross-section, the largest slope will occur halfway

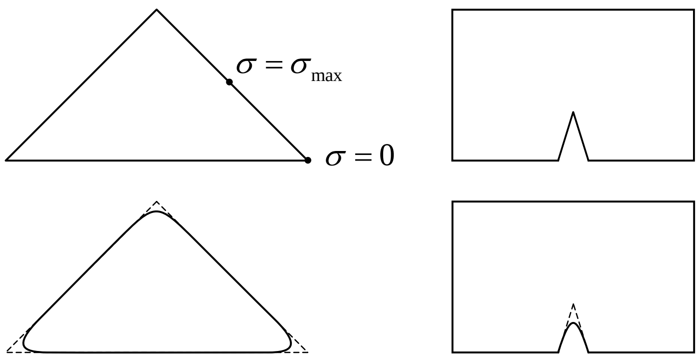

Fig. 6.26: membrane analogy as mental experiment to optimize cross-sections.

the sides of the triangle. At those positions the shear stress reaches its maximum. In the vertices, the soap film will be practically horizontal and no significant contribution to the moment and stiffness can be expected. Therefore, rounding off the vertices can save material. At the right side of Fig. 6.26, a notched rectangular cross-section is depicted. When the notch is sharp the contour lines will be concentrated around the tip of the notch and large stresses will occur. A blunt notch is much more favourable.

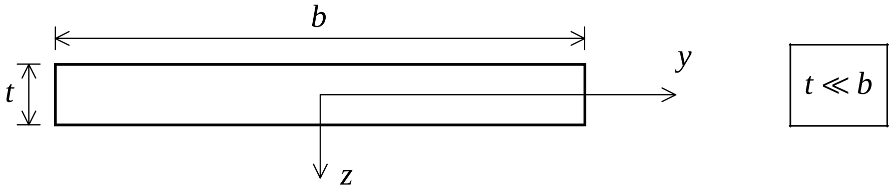

Fig. 6.27: Strip-shaped cross-section.

The mental experiment can be applied too for obtaining quantitative information. A well-known example is the torsion of a bar with a strip-shaped cross-section as shown in Fig. 6.27 (for this case, in previous lectures a solution was found already by a different method). When the experiment would be carried out with a membrane it can be expected that the deflection would be cylindrically shaped over practically the entire width b, independently of y. Only at the two ends $y = b/2$ and $y = -b/2$ a deviation from this shape would occur. For $t \ll b$ this will hardly affect the volume under the membrane, if it is assumed that the deflection w over the full width is only a function of z, see Fig. 6.28.

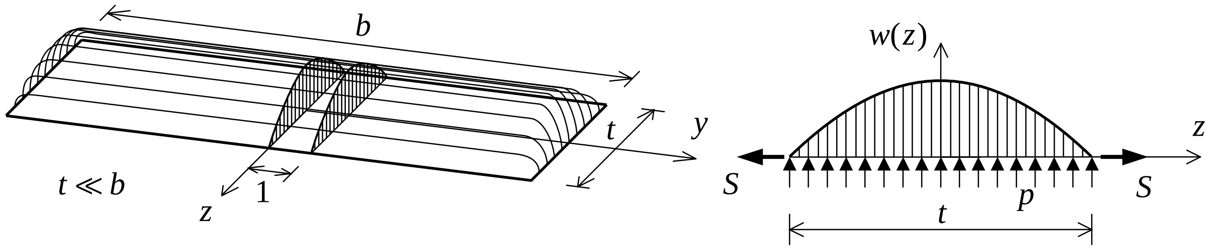

Fig. 6.28: Shape of the membrane for a strip-shaped cross-section.

The differential equation then simplifies to:

$$-\frac{1}{S}\frac{d^2w}{dz^2} = p$$

with boundary condition that w is zero for $z = \pm t/2$.
The solution for this equation is:

$$w(z) = \frac{p}{8S}t^2\left(1 - \frac{4z^2}{t^2}\right)$$

This is a parabola. In Fig. 6.23 it is shown that w is equivalent to ϕ, if at the same time it is substituted:

$$p = 2\theta \quad ; \quad s = \frac{1}{G}$$

Therefore, for the stress function ϕ it holds:

$$\phi(z) = \frac{Gt^2}{4}\left(1 - \frac{4z^2}{t^2}\right)\theta \tag{6.38}$$

This is a parabolic distribution with a maximum of:

$$\phi_{\max} = \frac{Gt^2}{4}\theta$$

The area between this parabola and the z-axis equals:

$$Area = \frac{2}{3} \times t \times \phi_{\max} = \frac{1}{6} G\, t^3 \theta \tag{6.39}$$

The torsional moment is twice the volume of the ϕ-bubble;

$$M_t = 2 \times b \times Area = \frac{1}{3} G\, b\, t^3 \theta$$

Since it also holds that:

$$M_t = GI_t\, \theta$$

For the torsional moment of inertia it is found:

$$I_t = \frac{1}{3} b\, t^3 \tag{6.40}$$

which already was indicated in Fig. 6.2.
Further, the stress distribution can be checked. In the direction of the long edge it holds:

$$\sigma_{xy} = \frac{\partial \phi}{\partial z} = -2Gz\theta \tag{6.41}$$

The maximum values in absolute sense occur for $z = \pm t/2$, see Fig. 6.29:

$$\sigma_{\max} = G\, t\theta$$

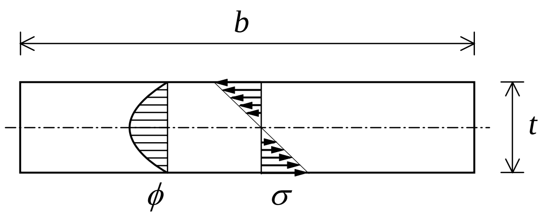

Fig. 6.29: Stress distribution in a strip-shaped cross-section.

With the aid of (6.39) this maximum stress can be expressed in the moment, an interesting relation for design purposes:

$$\sigma_{\max} = \frac{M_t}{\frac{1}{3} b t^2} \tag{6.42}$$

This expression was mentioned in Fig. 6.2 too.

Remarks

1. From the mental experiment it follows that the formula $I_t = \frac{1}{3} b t^3$ also can be used (in a similar approach) to determine the torsional moment of inertia of cross-sections, which are built up out of strip-shaped parts as shown in Fig. 6.30.

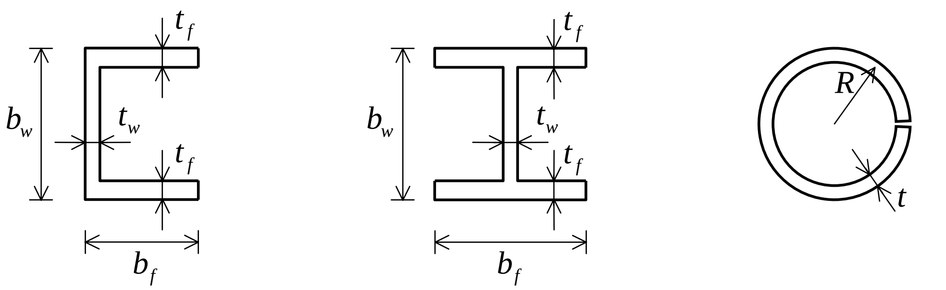

$$I_t = \frac{1}{3} b_w t_w^3 + \frac{2}{3} b_f t_f^3 \qquad I_t = \frac{1}{3} b_w t_w^3 + \frac{2}{3} b_f t_f^3 \qquad I_t = \frac{1}{3} b t^3 \ \text{ where } \ b = 2\pi R$$

Fig. 6.30: Torsional moments of inertia of thin-walled cross-sections.

2. The result for ϕ given by (6.38) leads to the stresses:

$$\sigma_{xy} = -\frac{M_t z}{\frac{1}{6} b t^3} \quad ; \quad \sigma_{xz} = 0$$

It was shown in general that the contribution to the moment of the stress σ_{xz} is the same as that of the stress σ_{xy}. However in this case this is not possible because σ_{xz} is zero. The share of the horizontal shear stresses σ_{xy} is correct:

$$-b \int_{-\frac{1}{2}t}^{\frac{1}{2}t} \sigma_{xy} z \, dz = \frac{M_t b}{\frac{1}{6} b t^3} \int_{-\frac{1}{2}t}^{\frac{1}{2}t} z^2 \, dz = \frac{1}{2} M_t$$

Nevertheless, in reality the missing part $M_t/2$ is delivered by vertical shear stresses σ_{xz}, which are present at the ends of the cross-section as shown in Fig. 6.31. At these ends the

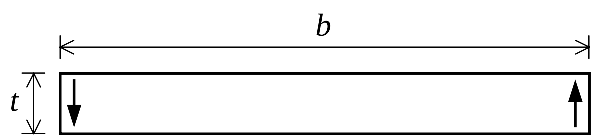

Fig. 6.31: Shear stresses at the ends contribute half of the torsional moment.

distribution of ϕ is not cylindrically in z but has to decrease to zero (see Fig. 6.28). These stresses are of the same order of magnitude as σ_{xy}, but because of the large distance between them (about b) they still produce half of the torsional moment M_t.

6.7 Numerical approach

The availability of fast computers makes it possible to generate numerical solutions. Suitable for this purpose is the Finite Element Method. A cross-section is divided into elements and in the nodes of the element mesh a value is determined for the displacement w of the membrane. It is a method of approximation, which produces more accurate results for finer meshes.

Strip-shaped cross-section

A very detailed discussion of this numerical method falls outside the scope of this course. Only the principle will be indicated and as an example the strip-shaped cross-section is taken, for which in section 6.6 already a solution has been determined. This solution will be labelled as the exact one. Since a cylindrically shaped displacement w is present, it is sufficient just to define an element distribution over the shortest edge t of the cross-section.

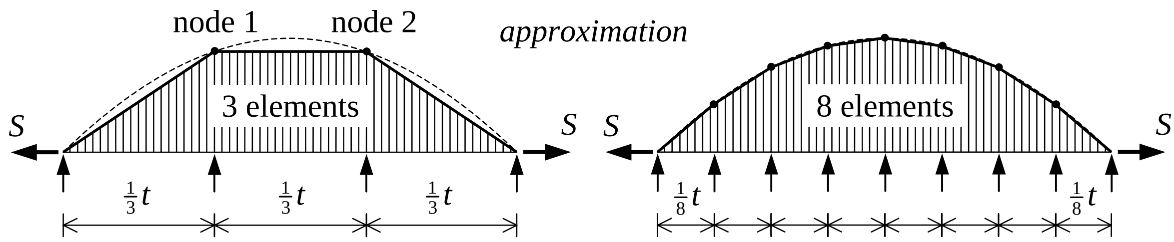

Fig. 6.32: Approximation of the shape of the membrane by three and eight elements.

The real distribution of the displacement $w(z)$ that is drawn by the dashed line in Fig. 6.32, is approximated by linear interpolation between two adjacent nodes. The figure shows the cases with three and eight elements. Now, the shape of the membrane is polygonal. With eight elements the approximation seems already to be quite good, but with three elements not yet. However for the coarse distribution with three elements the finite element method can be simulated by a calculation by hand. In the analysis, use will be made of the symmetry of the membrane surface. Fig. 6.33 shows the strip-shaped cross-section once more, including the section over the membrane. The uniformly distributed load p is concentrated as point loads F in the nodes at distances of $t/3$. The problem contains one degree of freedom w. This degree of freedom can be obtained from the equilibrium of node 1. After the determination of w, the torsional stiffness is calculated from the double volume beneath the membrane.
The calculation scheme of w is listed in Fig. 6.33. In node 1, the point load F has to be in equilibrium with the vertical component of the tension force S in the first element. Because w is small, $\tan\alpha$ can be replaced by the angle α itself and the displacement becomes:

$$w = \frac{t^2}{9S}\,p \tag{6.43}$$

The area of the section under the membrane over the full thickness t equals:

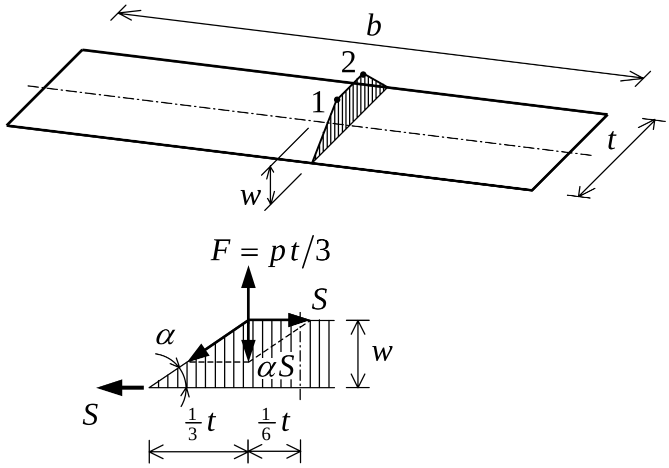

Concentrate : $F = \frac{1}{3} p t$ (1)

small w : $\alpha = \frac{w}{t/3}$ (2)

equilibrium of node 1 : $\alpha S = F$ (3)

substitution of (1) and (2) into (3):

$$\frac{3wS}{t} = \frac{1}{3} p t \quad \rightarrow \quad w = \frac{t^3}{9S} p$$

Fig. 6.33: Calculation of the displacement w for three elements.

$$Area = \frac{2}{3} w t$$

and the double volume:

$$2 \times Vol = 2 \times Area \times b = \frac{4}{3} w b t$$

Substitution of w from (6.43) yields:

$$2 \times Vol = \frac{4}{27} \frac{p}{S} b t^3$$

The ϕ-bubble is introduced by choosing:

$$p = 2\theta \quad ; \quad S = \frac{1}{G}$$

Then the double volume is equal to the torsional moment, and for $\theta = 1$ the result is the torsional stiffness GI_t:

$$GI_t = \frac{4}{27} \frac{2}{1/G} b t^3 = \frac{8}{27} G b t^3$$

The exact solution is:

$$GI_t = \frac{1}{3} G b t^3$$

The difference is in the order of 10 percent; for such a coarse element mesh this is quite a good result. The approximated solution appears to be exactly the inscribed polygon of the parabola.

In the computation with eight elements four different unknown displacements w occur. Then four equilibrium equations have to be set up and solved simultaneously. In that case, the error in GI_t already will be less than 1 percent.

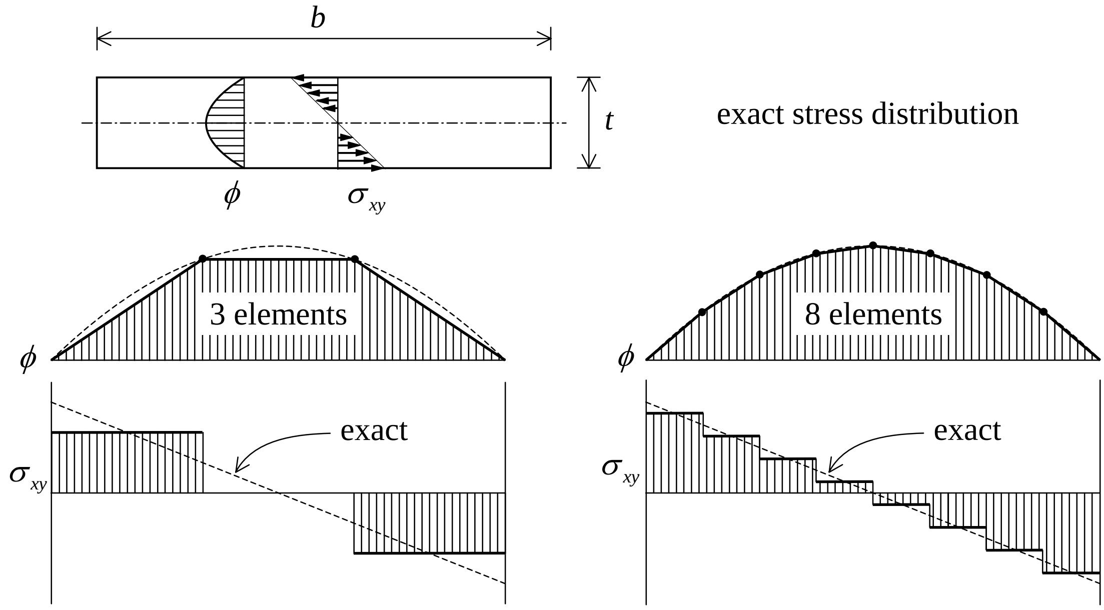

Fig. 6.34: Stress distribution obtained by finite element method.

The accuracy of the stress distribution is investigated as well. The exact solution is displayed in Fig. 6.34. Since ϕ is a parabolic function, its derivative the stress σ_{xy} will be linear over the thickness t of the cross-section. For a polygon description of ϕ with straight branches, the derivative will be constant per branch and will be discontinuous in the nodes. Fig. 6.34 shows the result that can be expected with the discussed finite element example. With three elements the largest error is not less than 33 percent, but for eight elements the error already reduces to 12 percent. In the middle of the elements always the correct value is found.

Arbitrarily shaped cross-sections

For arbitrarily shaped cross-sections a two-dimensional element mesh is applied. This can be done with triangular, rectangular and quadrilaterals of arbitrary shape (see Fig. 6.35). In the finite element approximation the load is again concentrated in the nodes. An unknown w (and therefore ϕ) is introduced in each node. Between the nodes, i.e. along the element edges the variation of w (and ϕ) is linear. Generally, the number of equations that can be formulated is equal to the number of nodes, thus equal to the number of unknown w's (and ϕ's). From this set the unknowns are solved.

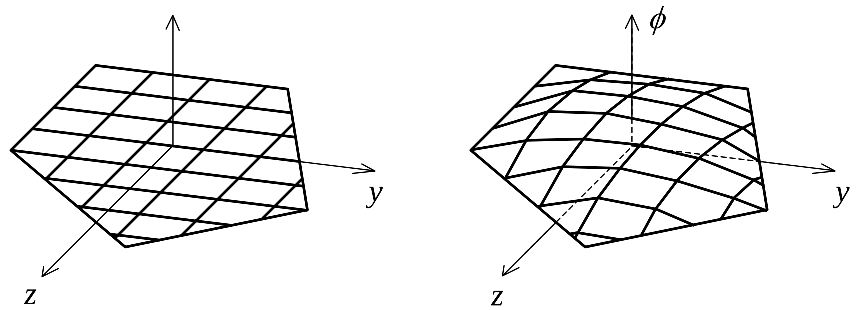

Fig. 6.35: Element mesh and ϕ-bubble for a cross-section of arbitrary shape.

Now, the ϕ-bubble is a collection of flat surfaces (above the triangular elements) and a collection of ruled surfaces (Dutch: “regelvlak”) (above the rectangular and quadrilateral elements). The formula read:

$$\phi(y,z) = a_1 + a_2 y + a_3 z \qquad (\textit{triangle})$$
$$\phi(y,z) = a_1 + a_2 y + a_3 z + a_4 yz \quad (\textit{rectangle})$$

The double content of the ϕ-bubble for $\theta = 1$ again provides the stiffness GI_t. The value of the stiffness is already quite good for relatively small numbers of elements. The stresses follow the slope of the ϕ-bubble. In a triangle both slopes $\phi_{,y}$ and $\phi_{,z}$ are constant over the entire element. The single value per element calculated for σ_{xy} and σ_{xz} is considered to be present in the centre of gravity of the element. In a rectangular element, each of the two slopes of ϕ is constant in one direction and linear in the other direction. This delivers two values for each of the stresses σ_{xy} and σ_{xz}. In an arbitrary quadrilateral the slopes vary in both directions and four values for σ_{xy} and σ_{xz} can be computed (see Fig. 6.36).

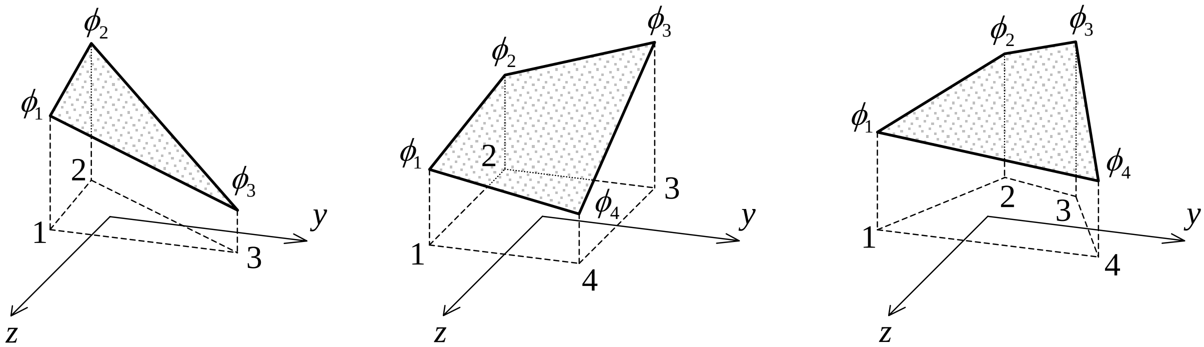

$\dfrac{\partial\phi}{\partial y}$ is constant — $\dfrac{\partial\phi}{\partial y}$ only varies in *z*-direction — $\dfrac{\partial\phi}{\partial y}$ varies in two directions

$\dfrac{\partial\phi}{\partial z}$ is constant — $\dfrac{\partial\phi}{\partial z}$ only varies in *y*-direction — $\dfrac{\partial\phi}{\partial z}$ varies in two directions

$\Downarrow$ $\Downarrow$ $\Downarrow$

one value for σ_{xy} — two values for σ_{xy} — four values for σ_{xy}

one value for σ_{xz} — two values for σ_{xz} — four values for σ_{xz}

Fig. 6.36: Stress distributions in the elements.

Increasing refinement of the mesh leads to better approximations approaching the exact solution. In Fig 6.37 this is demonstrated for a rectangular cross-section with a height-width ration of 2. When the number of elements $2N \times N$ increases, the ratio of the approximated and exact torsional stiffness GI_t approaches unity. This also holds for the maximum shear stress σ, provided it is evaluated halfway an elemental edge. When after a number of numerical tests it has become clear how fine the mesh should be for a particular accuracy, the calculation can be repeated for different height-width ratios. Then a table can be created as shown in Fig. 6.38. When $b \gg t$, the cross-section degenerates into a strip and for both GI_t and the maximum shear stress σ the coefficient $1/3$ is calculated, previously found in (6.40) and (6.42).

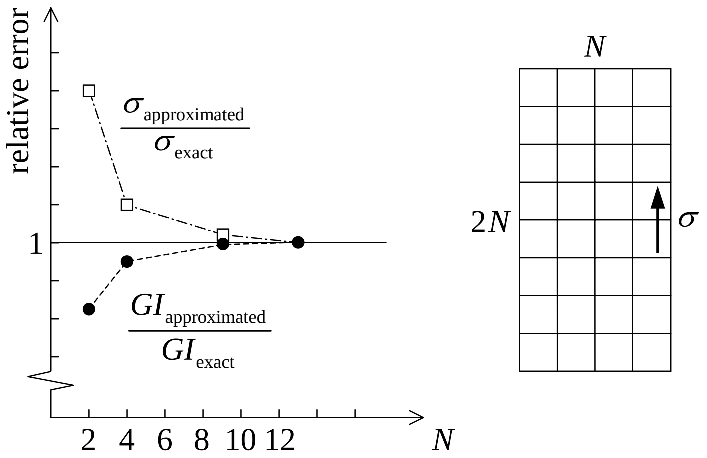

Fig. 6.37: Mesh refinement leads to convergence.

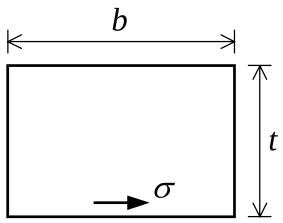

$\dfrac{b}{t}$	$\dfrac{GI_t}{bt^3G}$	$\dfrac{M_t}{\sigma b t^2}$
1.0	0.141	0.208
2.0	0.229	0.246
3.0	0.263	0.267
.	.	.
.	.	.
∞	0.333	0.333

Fig. 6.38: Stiffness and maximum stress for a rectangular cross-section.

6.8 Cross-section with holes

When the cross-section of the bar contains one or more cavities, the discussed theory requires some addition. First the case will be discussed with a single hole in the cross-section (see Fig. 6.39). Along the edge of the hole a n-s coordinate system is attached. The positive direction of n points into the hole. On the edge of the hole, no shear stress σ_{xn} different from zero can be present. Therefore it holds that:

$$\phi_{,s} = 0 \tag{6.44}$$

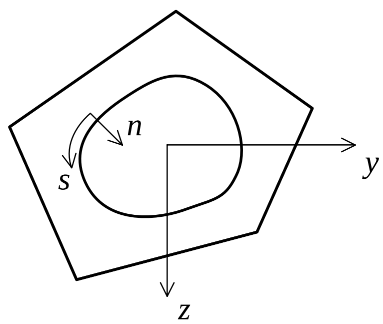

Fig. 6.39: Cross-section with one hole.

This means that ϕ is constant along the circumference of the hole. However in this case the value of ϕ cannot be set to zero, because this already has been done at the outer circumference. The unknown value is indicated by ϕ_h and is an undetermined degree of freedom of the problem.
The question arises which boundary condition for $\phi(y,z)$ has to be prescribed at the edge of the hole. The harmonic equation for ϕ is a second-order differential equation of the elliptic type, in which case generally only one boundary condition can be formulated on the edge. When this is the value of ϕ itself, one speaks about a Dirichlet problem as previously discussed. When the derivative $\phi_{,n}$ is prescribed the problem is of the Neumann type. Since at the outer circumference the value of ϕ was set to zero, at the edge of the hole ϕ is free and undetermined. Therefore, at that position the value of $\phi_{,n}$ has to be prescribed. Thus, the hole creates an extra unknown ϕ_h, which means that only one extra condition $\phi_{,n}$ has to be formulated along the edge of the hole, although $\phi_{,n}$ may vary itself along the circumference of the hole. It now will be investigated which condition this is. This will be done in two steps. First a special case is considered, for which the condition can be identified easily. After that it will be shown that this condition is generally valid.

Special case
Again the ϕ-bubble is considered occurring on a solid cross-section. In the left part of Fig. 6.40, the contour lines of the ϕ-bubble are indicated, i.e. the lines of constant ϕ. Along such a line the value of $\phi_{,s}$ is zero, which means that σ_{xn} is zero as well. This means that the part

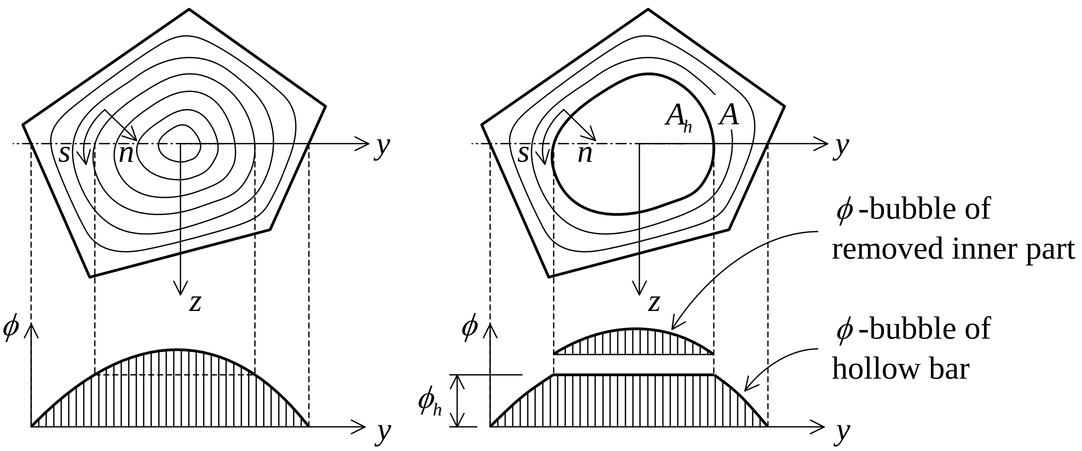

Fig. 6.40: Clarification on the ϕ-bubble of a cross-section with a hole.

of the bar inside the contour does not exert any force on the part outside the contour. Therefore, the inner part (with area A_h) can be removed without affecting the stress distribution outside the contour (with area A). This situation is depicted in the right part of Fig. 6.40. It also has been indicated how this affects the ϕ-bubble. For the solid cross-section a cut is made through the ϕ-bubble at the line $z = 0$. The contour line, inside which the hole will be created, intersects the curve twice with the same value for ϕ, namely ϕ_h.
In this case, the torsional stiffness GI_t for the hollow cross-section is equal to the difference of the torsional stiffness of the solid cross-section minus the torsional stiffness of the removed inner part. The cut-off cap of the ϕ-bubble represents the torsional stiffness of the removed part. It can be seen that for the ϕ-bubble of the hollow cross-section the hole continues to provide a contribution, but now with a constant value ϕ_h over the whole cavity. So, the

torsional stiffness is twice the volume of the truncated ϕ-bubble for $\theta = 1$, *including* the part above the hole. The formula reads:

$$\boxed{GI_t = 2\iint_A \phi \, \mathrm{d}A + 2\phi_h A_h \quad \text{for} \quad \theta = 1} \tag{6.45}$$

For further interpretation it make sense to investigate what impact above explanation has on the membrane analogy (see Fig. 6.41). This analogy still can be used if a small adaptation is included. Again the membrane is fixed at the outer circumference and spans the cross-section.

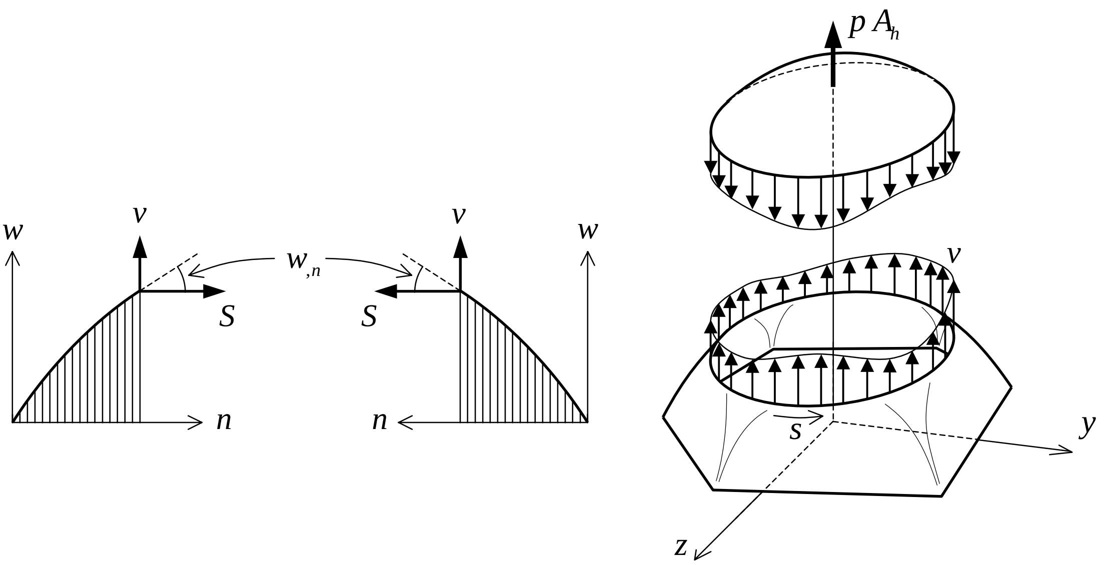

Fig. 6.41: The membrane analogy assists in finding the boundary condition for $\phi_{,n}$ along the hole.

On the edge of the hole the membrane is imaginarily fixed to a thin rigid weightless plate. This plate must be able to move freely. When a pressure p pressurises the membrane, it will load not only area A of the membrane with but also area A_h of the thin plate. Therefore, the weightless plate will be displaced parallel with respect to itself. The displacement of the membrane along the edge of the plate is the same and the slope with the plate is $w_{,n}$. The membrane analogy assists in finding the boundary condition for $\phi_{,n}$ along the circumference of the hole. For that purpose the equilibrium of the weightless plate is considered.
The weightless plate is subjected to a distributed load p over its surface and to the lateral membrane load v along the circumference. This lateral load has the value $S w_{,n}$ (n is positive if it points inside the hole). For the equilibrium of the weightless plate in w-direction it then can be written:

$$\oint v \, ds = p A_h \quad \rightarrow \quad \oint S \, w_{,n} \, ds = p A_h$$

When this result is reformulated in terms of the torsional problem ($p = 2\theta$, $S = 1/G$ and $w = \phi$), the required condition for $\phi_{,n}$ at the edge of the hole is found:

$$\oint \frac{1}{G}\phi_{,n}\, ds \quad = 2A_h\theta \tag{6.46}$$

General case

Now the idea is abandoned that a hole is created by removing material from a solid cross-section just inside a contour of the ϕ-bubble. In this case the hole is created arbitrarily and again a s-n coordinate system is attached along its circumference. Also the same boundary condition (6.44) holds and ϕ must have a constant value ϕ_h. In this case ϕ-contours are generated that generally do not correspond with those of the solid cross-section. This means that compared to the solid cross-section the stress distribution will be different. Therefore, it has to be proved separately that condition (6.46) holds for this case too. If so, the analogy of the weightless plate for the determination of the ϕ-bubble can be generalised. It also has to be shown that formula (6.45) for the determination of GI_t is generally valid.
Since $\phi_{,n}$ is equal to $-\sigma_{xs}$ and $\sigma_{xs} = G\gamma_{xs}$, condition (6.46) can be rewritten as:

$$\boxed{-\oint \gamma_{xs} ds \quad = 2A_h\theta} \tag{6.47}$$

In order to prove whether this contour integral is generally valid, it is investigated how γ_{xs} is expressed in the three-dimensional displacement field. This displacement field reads:

$$u_x(y,z) = \psi(y,z)\theta \quad ; \quad u_y(y,z) = -x\,z\,\theta \quad ; \quad u_z(y,z) = x\,y\,\theta \tag{6.48}$$

The shear angle γ_{xs} is defined by:

$$\gamma_{xs} = u_{x,s} + u_{s,x}$$

which means that the derivative in x-direction of the displacement $u_s(y,z)$ has to be determined. This displacement can be expressed in u_y and u_z as shown in Fig. 6.12:

$$u_s = -\sin\alpha\; u_y + \cos\alpha\; u_z$$

Then the required relation between γ_{xs} and the displacement field is found:

$$\gamma_{xs} = u_{x,s} - \sin\alpha\; u_{y,x} + \cos\alpha\; u_{z,x}$$

Substitution of (6.48) changes this result into:

$$\gamma_{xs} = \left\{ \psi_{,s}(y,z) + z\sin\alpha + y\cos\alpha \right\}\theta$$

So, the contour integral under investigation becomes:

$$-\oint \gamma_{xs} ds \quad = \left\{ -\oint \psi_{,s} ds - \oint z\sin\alpha\; ds - \oint y\cos\alpha\; dz \right\}\theta$$

Since $-\sin\alpha\, ds$ is just equal to dy and $\cos\alpha\, ds$ is just equal to dz this relation transforms into:

$$-\oint \gamma_{xs} ds = \left\{ -\oint \psi_{,s}\, ds + \oint z\, dy - \oint y\, dz \right\} \theta \tag{6.49}$$

The three contour integrals in the right-hand side will be determined separately. The first one can be written as:

$$\oint \psi_{,s}\, ds = \oint d\psi = 0$$

The value has to be zero because of the uniqueness of the warping displacement ψ along the circumference. The second integral equals:

$$\oint z\, dy = A_h$$

This result can easily be understood by splitting the integral into two parts. In the left part of Fig. 6.42 the contour integral is split into a part from A to B through the region with positive z-values and in a part from B to A with negative z-values. For the first part dy is positive

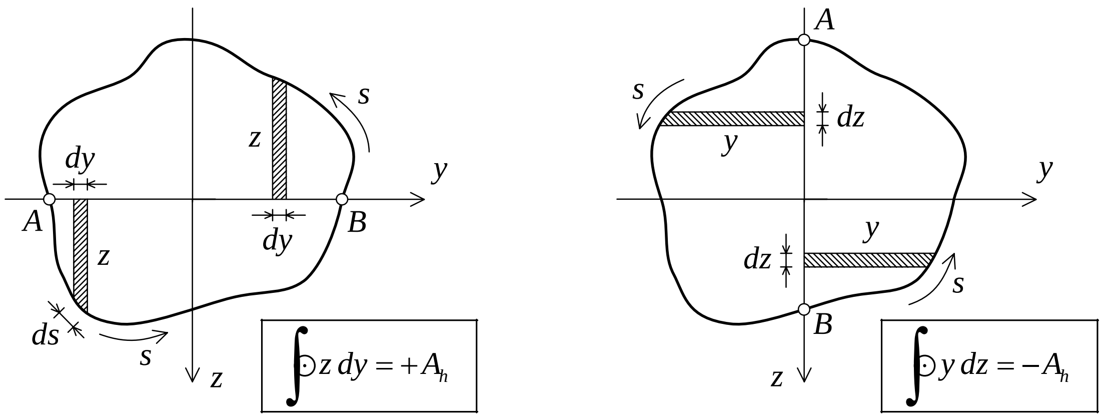

Fig. 6.42: Integrations of $\oint z\, dy$ *and* $\oint y\, dz$*.*

if s increases in positive direction and z is also positive in this area. Therefore, the integral over this part becomes:

$$\oint_{down} z\, dy = \textit{Area of the part of the hole for which } z \geq 0$$

In the second part of the contour integral dy is negative if s increases in positive direction, but z is negative as well, so that $z\,dy$ still is positive. Consequently, the integral over this part equals:

$$\oint_{up} z\, dy = Area\ of\ the\ part\ of\ the\ hole\ for\ which\ z < 0$$

The summation of both integrals just delivers the total area of the hole:

$$\oint z\, dy = \oint_{down} z\, dy + \oint_{up} z\, dy = A_h$$

Likewise, in the right part of Fig. 6.42 the area is split up into two parts for the third contour integral, a region where $y \geq 0$ and a region where $y < 0$. In a similar manner for the third contour integral it is found:

$$\oint y\, dz = \oint_{right} y\, dz + \oint_{left} y\, dz = -A_h$$

With these results for the three contour integrals, relation (6.49) transforms into:

$$-\oint \gamma_{xs}\, ds = 2A_h\, \theta$$

This is the same condition as found in (6.47) for the special case of a hole the edge of which coincides with a contour line of a solid cross-section. This means that it has been shown that this condition is valid too for an arbitrary position of the hole. So, the membrane analogy can also be applied for the determination of the ϕ-bubble. Only the plate will not automatically displace itself parallel to its original position and some sort of *guide* is required.

The only remaining aspect is to show that formula (6.45) retains its validity for the determination of the torsional stiffness GI_t from the ϕ-bubble. For the solid cross-section, the following relation was used:

$$GI_t = \iint_A \left(y\, \sigma_{xz} - z\, \sigma_{xy} \right) dA \quad \text{(for } \theta = 1\text{)}$$

or by expressing the stresses in ϕ:

$$GI_t = \iint_A \left(-y \frac{\partial \phi}{\partial y} - z \frac{\partial \phi}{\partial z} \right) dA \quad \text{(for } \theta = 1\text{)}$$

For the solid section, the integral over the area A was calculated in two parts. This will be done again, but now only that part of the area will be considered where material can be found (see Fig. 6.43).
The first integral can be worked out as follows:

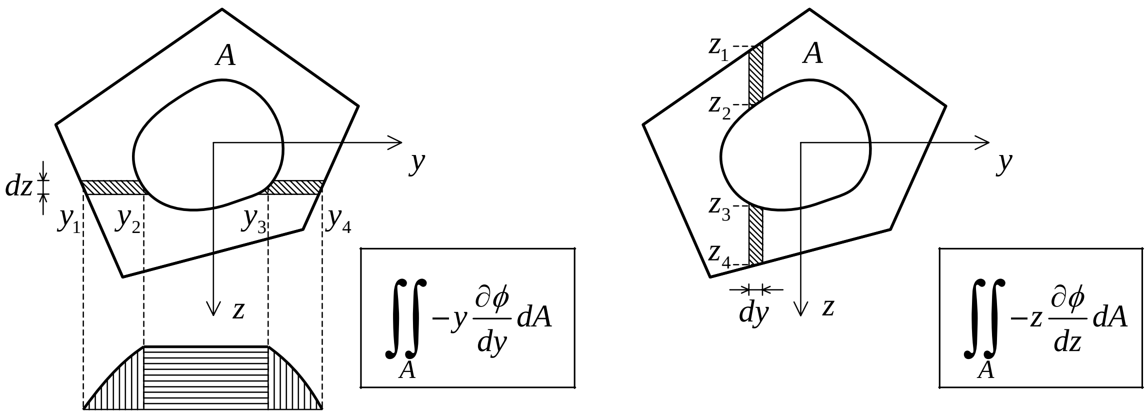

Fig. 6.43: Determination of the resulting moment for a cross-section with a hole.

$$\iint_A -y \frac{\partial \phi}{\partial y} dA = \int \left(\int_{y_1}^{y_2} -y \; d\phi + \int_{y_3}^{y_4} -y \; d\phi \right) dz$$

Integration by parts with respect to y changes this relation into:

$$\int \left(\int_{y_1}^{y_2} \phi \; dy - \left(y_2\phi_2 - y_1\phi_1 \right) + \int_{y_3}^{y_4} \phi \; dy - \left(y_4\phi_4 - y_3\phi_3 \right) \right) dz$$

On the outer circumference, ϕ_1 and ϕ_4 are zero, while ϕ_2 and ϕ_3 have the same value ϕ_h at the circumference of the hole. This reduces the integral to:

$$\int \left(\int_{y_1}^{y_2} \phi \; dy - \phi_h \left(y_3 - y_2 \right) + \int_{y_3}^{y_4} \phi \; dy \right) dz$$

The term between square brackets is just the area of the cross-section of the ϕ-bubble, including the part of the ϕ-bubble above the hole. Consequently it is found:

$$\iint_A -y \frac{\partial \phi}{\partial y} dA = \iint_A \phi \; dA + \phi_h A_h$$

Similarly it can be derived:

$$\iint_A -z \frac{\partial \phi}{\partial z} dA = \iint_A \phi \; dA + \phi_h A_h$$

For a cross-section with a hole it remains valid that the vertical and horizontal stresses contribute equally. Putting all results together it can be written:

$$GI_t = 2\iint_A \phi\, dA + 2\,\phi_h A_h = 2\iint_{A+A_h} \phi\, dA \quad (\text{for } \theta = 1)$$

This completes the proof that for any arbitrary position of the hole the torsional stiffness is equal to twice the volume of the ϕ-bubble, for $\theta = 1$.

Cross-section with a number of holes

It simply can be indicated how the calculation should be performed for more than one hole in the cross-section. In that case, the amount of unknown ϕ_h's is the same as the number of holes, and all these ϕ_h's may have a different value.

For the membrane analogy this means that above each hole a weightless plate is present, and that for each plate an equilibrium equation has to be formulated. When the shape of the membrane has been determined in this manner and the conversion of the torsional problem is carried out, the torsional stiffness can be determined from:

$$\boxed{GI_t = 2\iint \phi\, dA + 2\sum_{\text{all holes}} \phi_h A_h} \tag{6.50}$$

6.9 Thin-walled tubes with one cell

A special case of a cross-section with holes is a tube with a relatively small wall thickness. The circumference of the tube is C and it wall thickness t, such that $t \ll C$. Further it is assumed that the cross-sectional area inside the tube is equal to A_h.

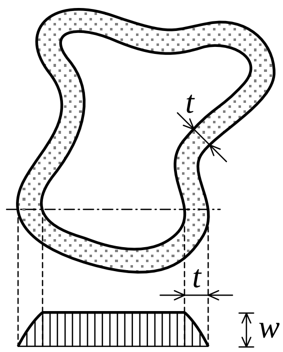

Fig. 6.44: Membrane for thin-walled tube.

According to the membrane analogy, the membrane and plate adjust themselves such that the plate elevates to a certain height w (see Fig. 6.44). Because t is very small, with a good approximation it can be assumed that the displacement of the membrane varies linearly from zero to w over the distance t. For the slope $w_{,n}$ it then holds:

$$w_{,n} = \frac{w}{t}$$

The equilibrium of the weightless plate is described by:

$$\oint S\, w_{,n}\, ds = p\, A_h$$

so that:

$$S \frac{w}{t} C = p\, A_h \quad \rightarrow \quad w = \frac{p}{S}\frac{t\, A_h}{C}$$

By substitution of $p = 2\theta$ and $S = 1/G$, the displacement w can be replaced by ϕ_h, i.e.:

$$\phi_h = 2G \frac{t\, A_h}{C}\theta$$

The torsional moment is twice the volume of the ϕ-bubble:

$$M_t = 2\iint_A \phi\, dA + 2\phi_h A_h$$

In this case, the area A of the material is equal to $t\,C$. For thin-walled tubes this area can be neglected with respect to the area of the hole A_h. The moment then becomes:

$$M_t = 2\phi_h A_h \quad \rightarrow \quad M_t = G \frac{4t\, A_h^2}{C}\theta$$

Therefore, the torsional moment of inertia becomes:

$$I_t = \frac{4t\, A_h^2}{C}$$

This formula is valid for a constant wall thickness t. When t varies along the circumference, the more general so-called *2nd formula of Bredt* holds:

$$\boxed{I_t = \frac{4A_h^2}{\oint \frac{ds}{t}}} \tag{6.51}$$

This formula follows from the equilibrium of the weightless plate. When t is constant, application of the formula leads to the above-derived relation for I_t. The shear stresses σ_{xs} are approximately constant across the thickness. Apart from the sign, it holds:

$$\sigma_{xs} = \frac{\phi_h}{t} = 2G \frac{A_h}{C}\theta$$

or expressed in the torsional moment:

$$\boxed{\sigma_{xs} = \frac{M_t}{2\,t\,A_h}} \tag{6.52}$$

This relation is called the *1st formula of Bredt.*

Remarks

1. The assumption that the membrane varies linearly over the wall thickness is an approximation. In reality a weak parabolic variation has to be added to the linear profile as shown in Fig. 6.45. This parabolic contribution represents the torsional moment of inertia

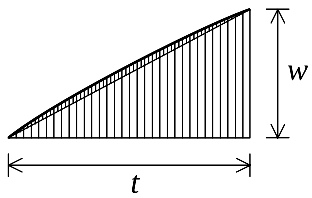

Fig. 6.45: Weakly curved membrane.

$\frac{1}{3}Ct^3$ of the wall itself, considered as a strip. However, compared to the torsional moment of the entire closed tube as a whole, the contribution of the wall can be neglected.

2. It is instructive to compare the results of a closed tube and an open tube (see Fig. 6.46).

closed tube	open tube
$I_t = 2\pi R^3 t$	$I_t = \frac{2\pi}{3} R t^3$
$\sigma_{\max} = \frac{M_t}{2\pi R^2 t}$	$\sigma_{\max} = \frac{1}{3}\frac{M_t}{2\pi R t^2}$

Fig. 6.46: Torsional stiffness of closed and open tubes.

The ratio of the stiffnesses is:

$$\frac{I_{closed\ tube}}{I_{open\ tube}} = 3\left(\frac{R}{t}\right)^2$$

The ratio of the stresses for the same moment equals:

$$\frac{\sigma_{closed\ tube}}{\sigma_{open\ tube}} = 3\left(\frac{t}{R}\right)$$

It can be seen that the stresses for the transmission of the same moment in the closed tube are an order t/R smaller than in the open tube, while the stiffness of the closed tube is much larger. This is caused by the fact that the "round-going" shear stresses in the closed tube have a large arm ($2R$), while this arm in the open tube is equal or smaller than t. This means that for the transmission of the same moment, in the last case the shear stresses are much larger.

6.10 Thin-walled tubes with multiple cells

In the building practice, it may be necessary to calculate the torsional stiffness of box-girders with more cells. An example with two cells is depicted in Fig. 6.47. The traffic arrangement on the upper deck of a bridge may be the cause that the vertical partitioning wall is applied

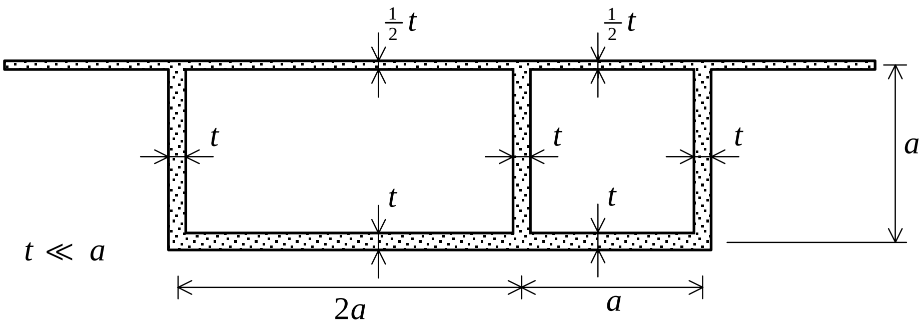

Fig. 6.47: Box-girder with two cells.

eccentrically. In this example, the thickness ($t/2$) of the upper deck is half the one (t) of the webs and the lower plate. Since $t \ll a$, the centre-to-centre distance (a and $2a$) of the box-girder walls can be used. This means that the contribution of the walls itself can be neglected. For the same reason, the flanges of the box-girder can be ignored as well.
Fig. 6.48 shows a cross-section of the membrane and the two weightless plates appearing in the membrane analogy. The left and right plate displace w_1 and w_2, respectively. In the drawing w_2 is chosen larger than w_1, which is consequently applied in the calculations as

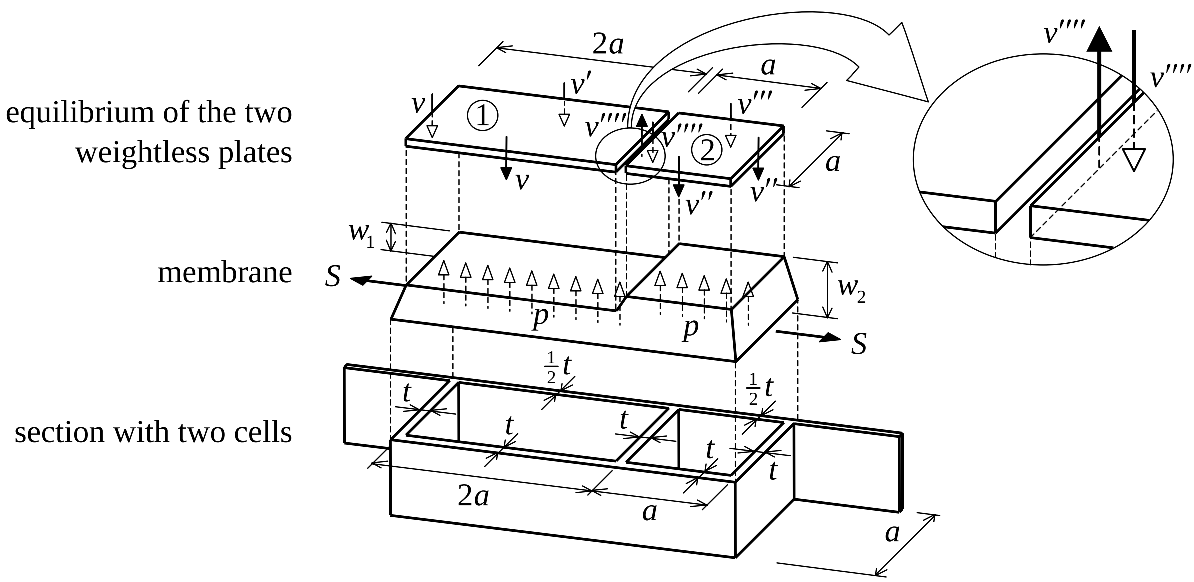

Fig. 6.48: Membrane and equilibrium of the plates.

well. The answers will reveal whether this assumption was correct. For the equilibrium of the two plates membrane shear forces of different magnitude play a role. When w_2 is larger than w_1, the shear forces as drawn in Fig. 6.48 will have a positive value. They are:

$$v = \frac{w_1}{t} S \quad ; \quad v' = \frac{w_1}{\frac{1}{2} t} S \quad ; \quad v'' = \frac{w_2}{t} S \quad ; \quad v''' = \frac{w_2}{\frac{1}{2} t} S \quad ; \quad v'''' = \frac{w_2 - w_1}{t} S$$

The first four shear forces v, v', v'' and v''' are applied in downward direction on the plates. The last force v'''' acts upward on plate 1 and downward on plate 2 (for the case of w_1 being larger than w_2 this is the other way round). The vertical equilibrium of the plates is:

$$\begin{aligned} &v * a \; + v * 2a \; + v' * 2a \; - v'''' * a \; = \; p * 2a * a \qquad (plate\ 1) \\ &v'' * a \; + v'' * a \; + v''' * a \; + v'''' * a \; = \; p * a * a \qquad (plate\ 2) \end{aligned}$$

Substitution of the forces provides:

$$\begin{aligned} &\frac{w_1}{t} S * a \; + \; \frac{w_1}{t} S * 2a \; + \; \frac{w_1}{\frac{1}{2} t} S * 2a \; - \; \frac{w_2 - w_1}{t} S * a \; = \; 2 p a^2 \qquad (plate\ 1) \\ &\frac{w_2}{t} S * a \; + \; \frac{w_2}{t} S * a \; + \; \frac{w_2}{\frac{1}{2} t} S * a \; + \; \frac{w_2 - w_1}{t} S * a \; = \; p a^2 \qquad (plate\ 2) \end{aligned}$$

Division by a changes this into:

$$\begin{aligned} 8 \frac{S}{t} w_1 \; - \; \frac{S}{t} w_2 \; &= \; 2 p a \qquad (plate\ 1) \\ -\frac{S}{t} w_1 \; + \; 5 \frac{S}{t} w_2 \; &= \; p a \qquad (plate\ 2) \end{aligned}$$

Solution of the two equations provides:

$$w_1 = \frac{11}{39} \frac{p}{S} a t \quad ; \quad w_2 = \frac{10}{39} \frac{p}{S} a t$$

The displacement w_2 is smaller than w_1. Therefore, the shear force v'''' is pointing in the opposite direction than it is drawn.
Now the transition is made to the ϕ-bubble by the introduction of $p = 2\theta$ and $S = 1/G$. This delivers:

$$\phi_1 = \frac{22}{39} G a t \theta \quad ; \quad \phi_2 = \frac{20}{39} G a t \theta$$

The torsional moment is twice the volume of the ϕ-bubble:

$$M_t = 2\phi_1 * 2a * a + 2\phi_2 * a * a \quad \rightarrow \quad M_t = \frac{128}{39} G a^3 t \theta$$

Obviously the torsional moment of inertia equals:

$$I_t = \frac{128}{39} a^3 t$$

Expressing ϕ_1 and ϕ_2 in the moment provides:

$$\phi_1 = \frac{11}{64}\frac{M_t}{a^2} \quad ; \quad \phi_2 = \frac{10}{64}\frac{M_t}{a^2}$$

For the stresses it then can be derived (see Fig. 6.49):

$$\sigma = \frac{\phi_1}{t} = \frac{11}{64}\frac{M_t}{ta^2} \quad ; \quad \sigma' = \frac{\phi_1}{\frac{1}{2}t} = \frac{22}{64}\frac{M_t}{ta^2} \quad ; \quad \sigma'' = \frac{\phi_2}{t} = \frac{10}{64}\frac{M_t}{ta^2}$$

$$\sigma''' = \frac{\phi_2}{\frac{1}{2}t} = \frac{20}{64}\frac{M_t}{ta^2} \quad ; \quad \sigma'''' = \frac{\phi_1 - \phi_2}{t} = \frac{1}{64}\frac{M_t}{ta^2}$$

Fig. 6.49 indicates the proper directions of the shear stresses. The first one can be chosen, and considering the slope of the membrane the other ones can be indicated. The partitioning has the same slope as the right web, which means that σ'''' points in the same direction as σ''.

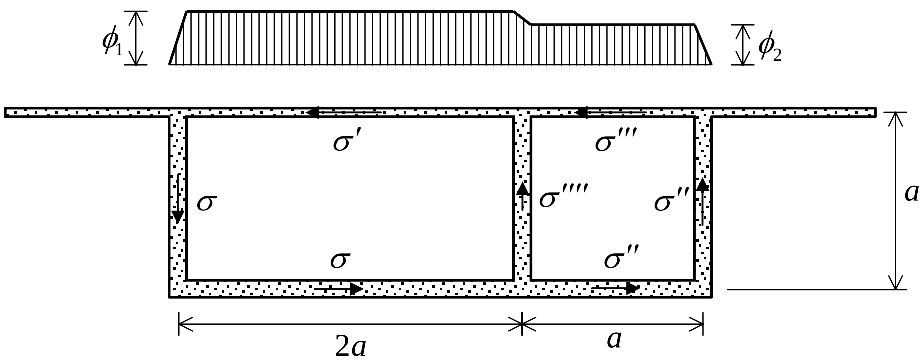

Fig. 6.49: ϕ-distribution and shear stresses in a section with two cells.

Exercises

1. Confirm that the resulting horizontal and vertical shear forces are zero in the discussed box-girder with two cells.
2. Check if the calculated vertical stresses deliver a torsional moment of $M_t/2$. Repeat the same exercise for the horizontal stresses.
3. Calculate with the formula of Bredt the torsional moment of inertia I_t and the stresses σ when the partitioning is left out of the structure. Compute the ratio of the I_t's and the maximum σ's for the situation with and without partitioning. What can be concluded?

6.11 Cross-section built up out of different materials

A cross-section composed out of two different materials A and B is considered as shown in Fig. 6.50. For these materials the respective shear moduli G_A and G_B are applicable. A n-s coordinate system is attached to the joining line, of which the s-coordinate is following the line and the n-coordinate is perpendicular to it. Now the boundary conditions along the

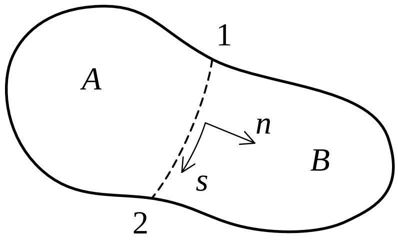

Fig. 6.50: Cross-section with two different materials A and B.

joining line are investigated. In Fig. 6.51 the n-direction is considered. The stress σ_{xn} has to be continuous across the joining line, because the stress σ_{xn} is transmitted from one material to the other. For the ϕ-bubble this means that the derivative $\partial\phi/\partial s$ has to be continuous. In both materials A and B, ϕ starts with zero value in edge point 1. Therefore, ϕ has to be continuous along the entire joining line.

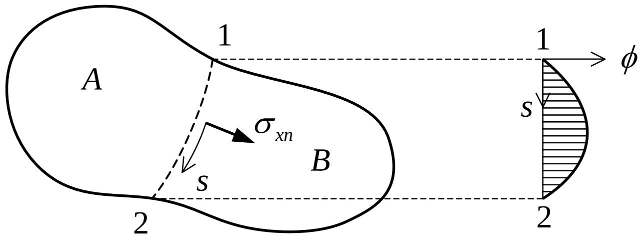

$$\boxed{\sigma_{xn_A} = \sigma_{xn_B}} \quad \Rightarrow \quad \frac{\partial\phi}{\partial s} = \text{CONTINUOUS} \quad \Rightarrow \quad \boxed{\phi = \text{CONTINUOUS}}$$

Fig. 6.51: Stress condition perpendicular to a connection line of two materials.

In Fig. 6.52 the s-direction is considered. In that direction the deformation condition holds that the shear strain γ_{xs} on the joining line is the same for both materials. Consequently, the stress σ_{xs} is discontinuous across the joining line (because the shear moduli G_A and G_B are different), this means that the slope $\phi_{,n}$ of the ϕ-bubble is discontinuous too. Therefore the ϕ-bubble contains a kink.
In the membrane analogy, the same procedure as described before can be followed. Only the tensile force for both materials is different. So, distinction has to be made between S_A and

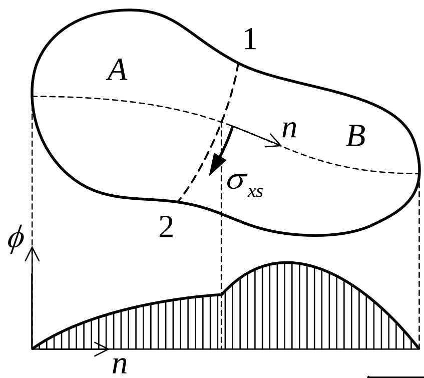

$$\boxed{\gamma_{xs_A} = \gamma_{xs_B}} \quad \Rightarrow \quad \sigma_{xs} = \text{DISCONTINUOUS} \quad \Rightarrow \quad \boxed{\frac{\partial\phi}{\partial n} = \text{DISCONTINUOUS}}$$

Fig. 6.52: Strain condition in the direction of a connection line of two materials.

S_B. This implicates again that a kink is created in the membrane. The shear force v_n must be continuous and because it holds that $v_n = S\,w_{,n}$ the slope $w_{,n}$ will be discontinuous for $S_A \neq S_B$.

Cross-section with hole as a special case

A cross-section with a hole can be regarded as a special case of a cross-section composed out of two materials. The hole is considered to be a special material with G equal to zero. Then

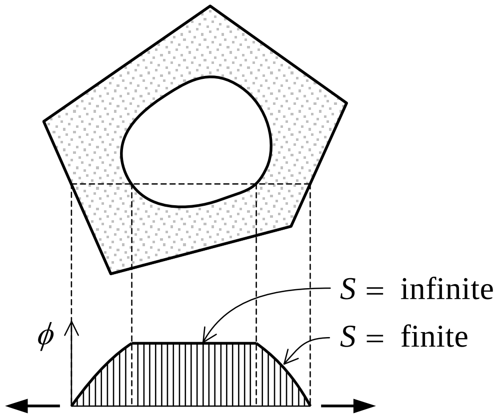

Fig. 6.53: Cross-section with a hole considered as a special case of two materials.

in the membrane analogy the tensile force S above this hole is infinitely large. Therefore, this part of the membrane remains flat (see Fig. 6.53). Making further use of the knowledge that:

$$\sigma_{xn_A} = \sigma_{xn_B} = 0 \quad \rightarrow \quad \phi_{,s} = 0 \quad \rightarrow \quad \phi_h = \text{constant}$$

Additionally it can be concluded that this flat part of the membrane remains horizontal. So, exactly the same goal is achieved as with the concept of a weightless plate!

6.12 Torsion with prevented warping

Up to now it has been assumed continuously that the ends of the bar were loaded in such a manner that no axial normal stresses σ_{xx} could be generated. An eventual warping of the cross-section could take place without any hindrance. However, if the warping at the end is prevented, for example by bonding the end to an undeformable body, a kinematic boundary condition is prescribed. Then it is not possible to prescribe zero stress values. So, generally normal stresses σ_{xx} will be generated. The influence of the prevented warping can be considerable. Especially the stiffness can be increased strongly. This can be demonstrated for example by the torsion of an I-section. When an I-section is subjected to torsion, the cross-

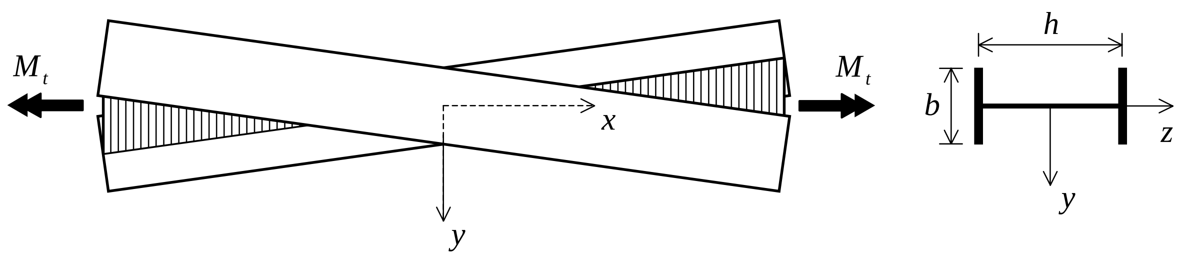

Fig. 6.54: Torsion of an I-section.

section warps. In each cross-section, the upper and lower flanges have opposite rotation directions as shown in Fig. 6.54. The right part of the section is drawn again in Fig. 6.55, but rotated over an angle of 90^0. At the left sketch the warping is free at the right sketch it is prevented. The prevention of the warping can be achieved by subjecting the top flange to a moment about the z-axis, while at the same time the bottom flange experiences a moment of the same magnitude but opposite direction. In both flanges this moment disappears gradually as the distance from the fixed end increases. These moments go together with shear forces V in y-direction in the flanges.

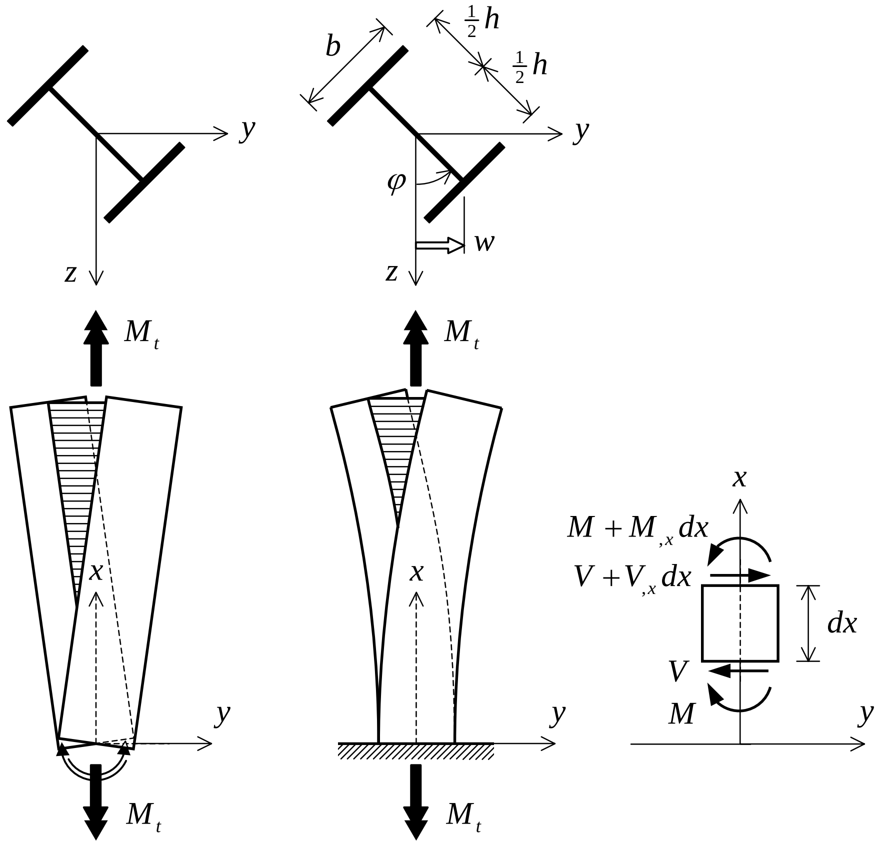

Fig. 6.55: I-section the warping of which is prevented.

The total torsional moment M_t is not only taken up by a “round-going” shear stream according to De Saint-Venant, but can partly be attributed to these shear forces V too (see Fig. 6.56). At the clamped end ($x = 0$), the warping is completely prevented. At that position, θ is zero and the moment is completely determined by Vh. For sufficiently large x it can be expected that V damps out to zero value and that θ has developed completely, so that at that position the torsional moment is resisted just as in the case of free warping ($GI_t\theta$).

The expected picture will now be worked out quantitatively. The rotation of the cross-section is equal to φ and the displacement of the top flange in y-direction is called w. The moment M and shear force V in this flange as drawn in Fig. 6.55 are considered positive. The following relations are valid:

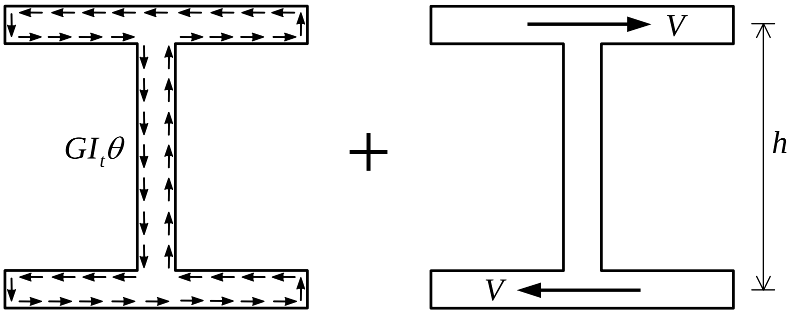

$$\boxed{M_t = GI_t\theta + V\,h}$$

Fig. 6.56: Shear forces V due to prevented warping.

$$\left.\begin{array}{l} \left.\begin{array}{l} V = \dfrac{dM}{dx} \\[2ex] M = -EI_f\,\dfrac{d^2w}{dx^2} \end{array}\right\} \;\rightarrow\; V = -EI_f\,\dfrac{d^3w}{dx^3} \\[6ex] \left.\begin{array}{l} w = \dfrac{h}{2}\varphi \\[2ex] \theta = \dfrac{d\varphi}{dx} \end{array}\right\} \;\rightarrow\; \dfrac{d^3w}{dx^3} = \dfrac{h}{2}\dfrac{d^2\theta}{dx^2} \end{array}\right\} \;\rightarrow\; V = -\frac{h}{2}EI_f\,\frac{d^2\theta}{dx^2}$$

where EI_f is the bending stiffness of a flange for bending in the plane of the flange. For the torsional moment it then follows:

$$M_t = GI_t\,\theta + V\,h \quad\rightarrow\quad M_t = GI_t\,\theta - \frac{1}{2}h^2 EI_f\,\frac{d^2\theta}{dx^2}$$

This is a differential equation in the unknown θ. After division by GI_t and the introduction of the characteristic length λ and the specific torsion angle θ_{sv} according to De Saint-Venant given by:

$$\lambda^2 = \frac{h^2 EI_f}{2GI_t} \quad ; \quad \theta_{sv} = \frac{M_t}{GI_t}$$

the differential equation becomes:

$$\theta - \lambda^2\,\frac{d^2\theta}{dx^2} = \theta_{sv}$$

The solution consists out of a particular and a homogeneous part:

$$\begin{array}{ll} \theta(x) = \theta_{sv} & (\textit{particular part}) \\ \theta(x) = C_1\,e^{x/\lambda} + C_2\,e^{-x/\lambda} & (\textit{homogeneous part}) \end{array}$$

The total solution is:

$$\theta(x) = \theta_{sv} + C_1\, e^{x/\lambda} + C_2\, e^{-x/\lambda}$$

The coefficient C_1 has to be zero, because the specific torsional angle $\theta(x)$ has to approach the value θ_{sv} for $x \to \infty$. Then the influence of the bonded end should not be felt anymore. The constant C_2 can be found from the condition that θ is zero for $x = 0$, i.e.:

$$x \to \infty:\ C_1 = 0 \quad ; \quad x = 0:\ C_2 = -\theta_{sv}$$

Therefore, the solution becomes:

$$\theta(x) = \left(1 - e^{-x/\lambda}\right)\theta_{sv}$$

On basis of this solution all desired stresses can be calculated. In Fig. 6.57 it can be seen that the influence of the fixed end is practically damped out at a distance of 2λ to 3λ.

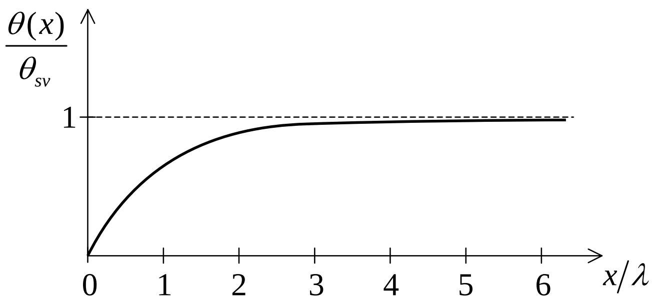

Fig. 6.57: Influence of the clamped end.

Example

For the sake of simplicity, Poisson's ratio υ is set to zero, so that $G = E/2$.
For an I-section with the same thickness for the web and the flanges it holds:

$$I_f = \frac{1}{12} t\, b^3 \quad ; \quad I_t = \frac{1}{3}(h + 2b)t^3$$

where b is the width of the flange. It then follows:

$$\frac{\lambda}{h} = \frac{b}{2t}\sqrt{\frac{b}{h + 2b}}$$

For more or less equal b and h, this relation becomes:

$$\frac{\lambda}{h} \approx \frac{1}{2\sqrt{3}}\frac{b}{t}$$

When b is much larger than t, then λ is much larger than h. The influence of the disturbance by the bonded end is noticeable up to a distance (about 3λ), which is much larger than the size (h) of the disturbed cross-section. In this case, the principle of de Saint-Venant appears not to be applicable. This means that the principle has no general validity.

A practical example of disturbed warping occurs in the case of viaducts built up out of pre-stressed beams, on which a high-lying deck is cast (see Fig. 6.58). The disturbance occurs at the end cross-members and eventual intermediate cross-members. Both b and h are of the

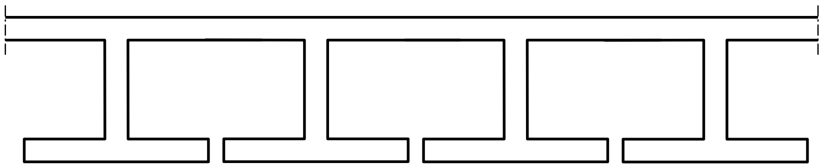

Fig. 6.58: Pre-stressed beam for viaduct.

order of magnitude of 1 m, while t is in the order of 0.20 m. With $b/t = 5$ the characteristic length becomes:

$$\lambda = \frac{5}{2\sqrt{3}} \approx 1.5 \text{ m}$$

a damping length of about 3λ provides more than 4 m. Compared to a span of 30 to 40 m this is a small part of the entire span. This means that the torsional stiffness of such a viaduct obtained through De Saint-Venant is sufficiently accurate, in case only end cross-members are applied. When intermediate cross-members are applied as well, the actual stiffness will be larger.